A Neural Model of how Horizontal and Interlaminar Connections of Visual Cortex Develop into Adult Circuits that Carry Out Perceptual Grouping and Learning

Stephen Grossberg and James R. Williamson

Department of Cognitive and Neural Systems and Center for Adaptive Systems, Boston University, Boston, MA 02215, USA

A neural model suggests how horizontal and interlaminar connections in visual cortical areas V1 and V2 develop within a laminar cortical architecture and give rise to adult visual percepts. The model suggests how mechanisms that control cortical development in the infant lead to properties of adult cortical anatomy, neurophysiology and visual perception. The model clarifies how excitatory and inhibitory connections can develop stably by maintaining a balance between excitation and inhibition. The growth of long-range excitatory horizontal connections between layer 2/3 pyramidal cells is balanced against that of short-range disynaptic interneuronal connections. The growth of excitatory on-center connections from layer 6-to-4 is balanced against that of inhibitory interneuronal off-surround connections. These balanced connections interact via intracortical and intercortical feedback to realize properties of perceptual grouping, attention and perceptual learning in the adult, and help to explain the observed variability in the number and temporal distribution of spikes emitted by cortical neurons. The model replicates cortical point spread functions and psychophysical data on the strength of real and illusory contours. The on-center, off-surround layer 6-to-4 circuit enables top-down attentional signals from area V2 to modulate, or attentionally prime, layer 4 cells in area V1 without fully activating them. This modulatory circuit also enables adult perceptual learning within cortical area V1 and V2 to proceed in a stable way.

Introduction

A central question in neuroscience concerns how the visual cortex autonomously develops, stabilizes its own development and then gives rise to visual perception in the adult. A neural model is presented of how these processes work and are related. The model suggests how the mechanisms that enable development to stabilize in the infant lead to adult properties of perceptual grouping, attention and learning. It hereby opens a path towards unifying three fields: infant cortical development, adult cortical neurophysiology and anatomy, and adult visual psychophysics.

A related question concerns why visual cortex, indeed all neocortex, is organized into layers. What functional properties are achieved by 'laminar computing'? The model clarifies how such laminar computing abets both infant development and adult perception by enabling cortex to select and complete correct groupings of visual signals, while actively suppressing incorrect groupings, without losing sensitivity to the relative contrasts and spatial positions of these signals.

The model proposes developmental rules whereby cortical circuits grow whose excitatory and inhibitory signals are balanced. Several model studies have shown how balanced excitation and inhibition can produce the highly variable interspike intervals that are found in cortical data (Shadlen and Newsome, 1998; van Vreeswijk and Sompolinsky, 1998). The present study suggests that such variability may reflect mechanisms that are needed to ensure stable development and learning by cortical circuits.

Cells in cortical area V1 are arranged into columns whose local circuits link together cortical layers. Cells in each column have similar orientational tuning and sensitivity to eye of origin, or ocular dominance. The columns are arranged into two-dimensional maps of orientation and ocular dominance (Hubel and Wiesel, 1962, 1963, 1968). Cortical simple cells are sensitive to the contrast polarity of oriented image contrasts, whereas complex cells pool signals from like-oriented opposite contrast polarities. The classical, oriented receptive fields of these cells are derived from local interactions between cells in nearby cortical columns. A number of models have studied how simple cells and complex cells develop their orientationally tuned receptive fields within maps of orientation and ocular dominance (von der Malsburg, 1973; Grossberg, 1976a; Willshaw and von der Malsburg, 1976; Swindale, 1980, 1982, 1992; Linsker, 1986a, 1986b; Rojer and Schwartz, 1989, 1990; Durbin and Mitchison, 1990; Obermayer *et al.*, 1990, 1992; Miller, 1992, 1994; Grossberg and Olson, 1994; Sirosh and Miikkulainen, 1994; Olson and Grossberg, 1998) [these models have been reviewed by Olson and Grossberg (Olson and Grossberg, 1998)].

None of the models has investigated the functional utility of organizing visual cortex into layers. Nor have they modeled development of the longer-range horizontal and interlaminar interactions that link cells in different cortical columns, or how such development may be stabilized by self-balancing excitatory and inhibitory signals. These interactions are often cited as the basis of 'non-classical' receptive fields that are sensitive to the context in which individual features are found (von der Heydt *et al.*, 1984; Peterhans and von der Heydt, 1989; Born and Tootell, 1991; Knierim and van Essen, 1992; Sillito *et al.*, 1995). The present article assumes that receptive fields of individual simple and complex cells have already substantially developed in their respective layers and columns, and models how longer-range horizontal and interlaminar connections develop between columns. This type of study extends the functional understanding of cortical organization, because the perceptual units that visual cortex processes are spatially distributed patterns of luminance or color that are processed in parallel by multiple, interacting columns. The model was briefly reported previously (Grossberg and Williamson, 1997; Williamson and Grossberg, 1998).

Methods

Linking Cortical Development to Adult Perception

Perceptual grouping is the process whereby the brain organizes image contrasts into emergent boundary structures that segregate objects and their backgrounds in response to texture, shading and depth cues in scenes and images (Julesz, 1971; Ramachandran and Nelson, 1976; Beck *et al.*, 1983; Polat and Sagi, 1994). Perceptual grouping is a basic step in

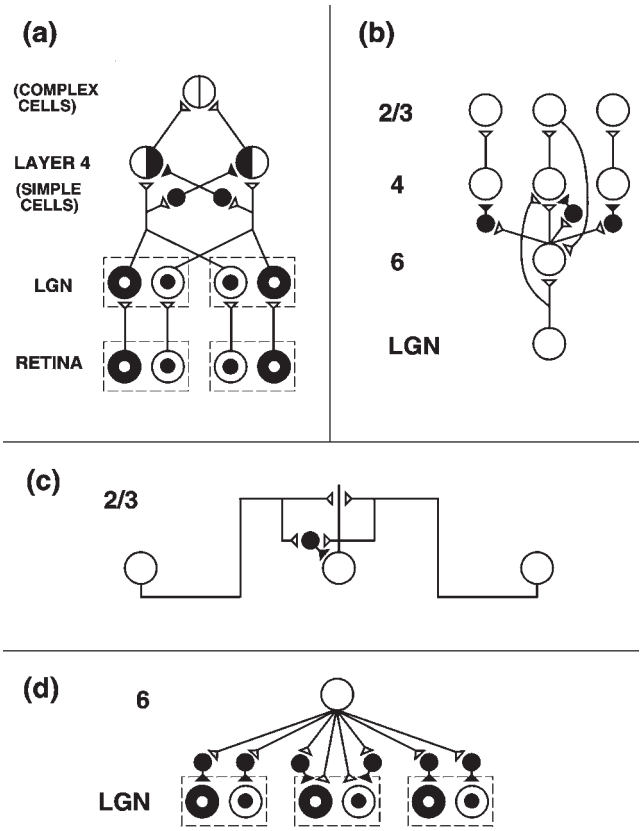

Figure 1. The adult network of retinal, V1 and lateral geniculate nucleus (LGN) neurons to which the developmental model converges. (*a*) Feedforward circuit from retina to LGN to cortical layer 4. Retina: retinal ON cells have on-center off-surround organization (white disk surrounded by black annulus). Retinal OFF cells have an off-center on-surround organization (black disk surrounded by white annulus). LGN: the LGN ON and OFF cells receive feedforward ON and OFF cell inputs from the retina. Layer 4: LGN ON and OFF cell excitatory inputs to layer 4 establish oriented simple cell receptive fields. Like-oriented layer 4 simple cells with opposite contrast polarities compete before generating half-wave rectified outputs. Pooled simple cell outputs enable complex cells to respond to both polarities. They hereby full-wave rectify the image. See text for details. (*b*) Cortical feedback loop between layers 4, 2/3 and 6: LGN activates layer 6 as well as layer 4. Layer 6 cells excite layer 4 cells with a narrow on-center and inhibit them using layer 4 inhibitory interneurons that span a broader off-surround. Layer 4 cells excite layer 2/3 cells, which send excitatory feedback signals back to layer 6 cells via layer 5 (not shown). Layer 2/3 can hereby activate the feedforward layer 6-to-4 on-center off-surround network. (*c*) The horizontal interactions in layer 2/3 that initiate perceptual grouping: layer 2/3 complex pyramidal cells monosynaptically excite one another via horizontal connections, primarily on their apical dendrites. They also inhibit one another via disynaptic inhibition that is mediated by model smooth stellate cells. (*d*) Top-down corticogeniculate feedback from layer 6: LGN ON and OFF cells receive topographic excitatory feedback from layer 6, and more broadly distributed inhibitory feedback via LGN inhibitory interneurons that are excited by layer 6 signals. The feedback signals pool outputs over all cortical orientations and are delivered equally to ON and OFF cells.

Table 1
Diagram of model connections

Equations	Source		Target	Sign	Kernel	Learning equation
(1)–(3)	Input	⇒	R	E or I	1	–
	Input	⇒	R	E or I	$G(\sigma_1)$	–
(4)–(7)	R	⇒	L	E	1	–
	6E	⇒	L	E	1	–
	6E	⇒	L	I	$G(\sigma_1)$	–
(8)–(13), (15)–(17)	L	⇒	S	E and I	$G(\sigma_2)$	–
(14)–(15)	S	⇒	C	E and I	1	–
(18)–(19)	C	⇒	4E	E	1	–
	6E	⇒	4E	E	1	–
	4I	⇒	4E	I	W^+	(28)
(20)–(22)	C	⇒	6E	E	1	–
	2/3E	⇒	6E	E	1	–
(23)	6E	⇒	4I	E	1	–
	4I	⇒	4I	I	W^-	(27)
(24)–(25)	4E	⇒	2/3E	E	1	–
	2/3E	⇒	2/3E	E	H (U V)	(31), (35)
	2/3I	⇒	2/3E	I	T^+	(38)
(26)	2/3E	⇒	2/3I	E	$H(UV)$	(31), (35)
	2/3I	⇒	2/3I	I	T^-	(37)

The first columns lists equations describing the model dynamics for each type of target cell. The second column lists the relevant source and target cells, with the sign of their interaction listed in the third column. Key: R, retina; S, simple cells; C, complex cells; 6, layer 6; 4, layer 4; 2/3, layer 2/3; E, excitatory; I, inhibitory. The fourth column lists the interaction kernels. Here, '1' means a point-to-point connection, i.e. to a cell in a different layer at the same position and (if applicable) with the same orientation preference. $G(\sigma)$ refers to a spatial Gaussian kernel with a standard deviation of σ. The remaining kernels, W^+, W^-, U, V, T^+ and T^-, are learned. These kernels are completely general, having both iso- and cross-orientational connections within their spatial extent. The final column lists the relevant learning equations next to these kernels.

solving the 'binding problem', whereby spatially distributed features are bound into representations of objects and events in the world. Illusory contours are a particularly vivid form of perceptual grouping, since they illustrate how perceptual groupings can form over image locations that contain no contrastive scenic elements.

The model suggests that many aspects of cortical design have evolved to carry out perceptual grouping. In particular, the model proposes how the laminar circuits of visual cortex enable it to develop connections capable of actively selecting and completing the perceptual grouping which best represents a visual scene, and suppressing the weaker groupings which represent the scene less well. The winning grouping that is chosen in this way can also represent the relative contrasts and spatial positions of objects in the scene.

Such a linkage between brain and behavior typically requires a demonstration of how interactions among many model cells give rise to emergent properties that match behavioral data. Several types of emergent properties are simulated by the model. The model assumes that the classical receptive fields of simple and complex cells have already developed. This hypothesis is consistent with data showing that the oriented pattern of lateral geniculate nucleus (LGN)-to-V1 connections develops prior to eye opening and structured visual input (Chapman *et al.*, 1991; Antonini and Stryker, 1993a; Chapman and Stryker, 1993). The model focuses upon how the longer-range non-classical connections between cortical columns develop both prior to eye opening and after structured visual inputs occur. We propose rules whereby such cortical development is controlled. Several such rules work together to control stable growth of model connections by ensuring that balanced excitatory and inhibitory connections develop. The emergent properties of this developmental process are the adult anatomical and neurophysiological circuits into which the model develops. After model development stabilizes, visual inputs activate cells within the developed anatomy, thereby leading to a second type of emergent properties, namely the cell activity patterns that match data about adult visual perception.

Classical Receptive Fields

The model assumes that three types of circuits with (primarily) classical receptive field properties develop, at least in part, before the circuits that subserve non-classical receptive fields. We call the circuits that have already developed 'pre-developed' circuits. The circuits that develop through model dynamics are called 'self-organized' circuits. The model analyzes one important combination of intracortical and intercortical pathways. It does not attempt to model all cortical connections, or the variations that exist across species. It also models the pre-developed circuits in the simplest possible way, since they are not the focus of the study, and the computational demands of the simulations are great even with these simplifications. Preliminary studies indicate, however, that the computational principles modeled herein can be elaborated and adapted to handle these variations.

Model analyses will be restricted to cortical area V1, and more particularly to the interblob organization of V1 that we propose interacts with area V2 to carry out perceptual grouping of boundary contours. Converging evidence suggests that area V2 replicates the structure of

area V1, but at a larger spatial scale (van Essen and Maunsell, 1983; von der Heydt *et al.*, 1984; Felleman and van Essen, 1991; Grosof *et al.*, 1993; Kisvarday *et al.*, 1995). We therefore assume that similar developmental processes may be operative in both V1 and V2. The model's predeveloped and self-organized properties are described below, first intuitively and then mathematically. Figure 1 and Table 1 schematize the model's connections. The proposed role of the blob stream in forming surface representations, and its predicted interactions with the boundaries formed in the interblob stream, are discussed elsewhere (Gove *et al.*, 1995; Grossberg, 1994, 1997; Grossberg and McLoughlin, 1997; Grossberg and Pessoa, 1998).

Direct LGN Inputs to Layer 4

In both the brain and the model, the retina activates the LGN, which, in turn, inputs to cortical area V1. LGN inputs directly excite layer 4C in both the cat and macaque, as well as layer 4A in the macaque (Hubel and Wiesel, 1962; Chapman *et al.*, 1991; Reid and Alonso, 1995). In the model, a single, generic, layer 4 is used for simplicity; see the pathways with open triangles in Figure 1*a*. These inputs play a key role in establishing the orientational tuning of V1 simple cells.

Simple cells in the brain respond to a given orientation and contrast polarity, i.e. they respond best to visual inputs that have a prescribed orientation and whose luminance preference, across this oriented axis, goes either from dark-to-light, or from dark-to-light, but not both. Simple cells in the model are pre-developed and are represented by circular symbols with half white and half black hemidisks in Figure 1*a*. Model simple cell properties arise as follows from model LGN inputs and intracortical interactions: LGN ON cells (cells that are turned on by input onset; see symbols with white disks and black annuli in Fig. 1*a*) and LGN OFF cells (cells that are turned off by input onset; see symbols with black disks and white annuli in Fig. 1*a*) both input to layer 4. They are organized into spatially offset arrays, with the ON cell inputs spatially displaced with respect to the OFF cell inputs, as in Figure 1*a*. Due to this input array, layer 4 simple cells can respond to an oriented input whose luminant area excites the ON cells, and whose dark area excites the OFF cells.

Selectivity of simple cell responses to oriented contrasts is improved by including mutually inhibitory interactions between cells that are sensitive to the same orientation but opposite contrast polarities (Palmer and Davis, 1981; Pollen and Ronner, 1981; Ferster, 1988; Liu *et al.*, 1992; Gove *et al.*, 1995); see the pathways with black triangles in Figure 1*a*. Then, when model cells that code opposite contrast polarities are equally activated by a uniform pattern of activation in the LGN, they shut each other off by mutual inhibition. On the other hand, when there is an oriented transition from ON to OFF activations in the LGN, the simple cells that best match its position, orientation and polarity will be most activated. Olson and Grossberg (Olson and Grossberg, 1998) have modeled how mutually inhibitory simple cells develop which are sensitive to the same orientation and opposite contrast polarities, at the same time that a cortical map develops whose orientation and ocular dominance columns exhibit the fractures, singularities and linear zones reported by others (Blasdel, 1992a; 1992b; Obermayer and Blasdel, 1993).

Balanced LGN Inputs to Layer 4 via Layer 6

In both brain and model, LGN inputs also directly excite layer 6 (Ferster and Lindström, 1985), which then indirectly influences layer 4 via an on-center off-surround network of cells (Grieve and Sillito, 1991a,b, 1995; Ahmed *et al.*, 1994, 1997). In both brain and model, cells in the on-center receive excitatory inputs from layer 6, whereas those in the spatially broader off-surround, which spans more than a single hypercolumn (Grieve and Sillito, 1995), receive inhibitory inputs from layer 6 via inhibitory interneurons in layer 4. In Figure 1*b*, open triangles designate excitatory connections and black triangles designate inhibitory connections. Such a combination of direct and indirect input pathways to layer 4 is found in many neocortical areas (van Essen and Maunsell, 1983; Felleman and van Essen, 1991). The model suggests that it helps to preserve stable development and learning in all these areas, while also allowing them to be activated by bottom-up inputs. In particular, the model predicts that the excitation and inhibition within the on-center of the 6-to-4 pathway are approximately balanced. The model also predicts that, if the on-center inputs from layer 6 get too strong relative to the off-surround inputs from layer 6 to 4, then development does not self-stabilize. Instead, the non-classical receptive fields of the model proliferate uncontrollably. On the other hand, if the inhibition gets too strong, then it can inhibit the inputs arriving at layer 4 too much, thereby preventing the cortex from becoming activated at all.

Maintaining a balance between the excitation and inhibition within the on-center from layer 6 to 4 has important implications for cortical design. Direct activation of layer 6 is predicted to modulate, prime or subliminally activate, cells in layer 4, but not to fire them vigorously. This prediction is consistent with the finding that layer 4 EPSPs elicited by layer 6 stimulation are much weaker than those caused by stimulation of LGN axons or of neighboring layer 4 sites (Stratford *et al.*, 1996), and also with the fact that binocular layer 6 neurons synapse onto monocular layer 4 cells of both eye types without reducing these cells' monocularity (Callaway, 1998, p. 56). Other compatible data have been reported (Hupé *et al.*, 1997; Wittmer *et al.*, 1997). We suggest that the on-center excitation is inhibited down into being modulatory by the overlapping and broader off-surround. Thus, although the center excitation is weak, the suppressive effect of the off-surround inhibition can be strong. The need to maintain the on-center excitatory–inhibitory balance also predicts why direct inputs to layer 4 are needed, in addition to the indirect on-center inputs via layer 6, in many cortical areas. The model predicts that, by themselves, the indirect 6-to-4 inputs cannot activate layer 4 cells without destabilizing cortical development and learning. Hence the direct bottom-up inputs to layer 4 are predicted to be necessary to initiate cortical firing.

Given that strong direct inputs from LGN to layer 4 do exist, the combined effect of both the direct and indirect pathways from LGN to layer 4 is to form an on-center off-surround network whose net on-center excitatory input can fully activate layer 4 cells. When cells in such a network obey the membrane equations of neurophysiology, they can maintain their sensitivity to input intensities that may vary over a large dynamic range (Grossberg, 1973, 1980b; Heeger, 1993; Douglas *et al.*, 1995). This is because the membrane equations contain 'shunting', or automatic gain control terms, that respond to properly balanced on-center and off-surround inputs by normalizing the activities of target cells without destroying their sensitivity to the relative sizes of the inputs. In the present instance, such a model network maintains the sensitivity of cells in layer 4 to inputs from the prior processing level, whether it be cells in V1 responding to LGN inputs, cells in V2 responding to inputs from V1, or any other combination of inputs. The layer 6-to-4 network is also used to preattentively select and attentively modulate the perceptual groupings that form in layer 2/3 (Grossberg, 1999; Grossberg and Raizada, 2000).

In summary, the model predicts that the mechanism whereby the balance between excitation and inhibition is maintained in the layer 6-to-4 circuit is of the greatest importance for achieving stable cortical development and later visual perception. This issue has hardly been explored experimentally. This prediction implies that a key cortical design problem is the following: as more and more cells in the off-surround become activated by increasingly dense patterns of inputs, what prevents the total inhibition that is converging on a layer 4 cell from growing linearly? If there was just enough inhibition to balance the excitation when just a few inputs were active, then why would not the inhibition become much too strong when many inputs were active, thereby shutting down the network? On the other hand, if the inhibition is well balanced when many inputs are active, then why does not runaway excitation occur when just a few inputs are active?

Development of Self-normalizing Inhibitory Interneurons in Layer 4

The model solves this problem by assuming that the inhibitory interneurons in layer 4 inhibit one another, as well as target cells in layer 4 [see Ahmed *et al.* (Ahmed *et al.*, 1994, 1997) for consistent data]. In particular, the model suggests how layer 4 inhibitory interneurons connect to layer 4 spiny stellate excitatory cells as well as to other nearby layer 4 inhibitory interneurons during development. These connections eventually span all the orientation columns within a hypercolumn, as well as all the orientation columns of neighboring hypercolumns. This recurrent inhibition converts the network of inhibitory interneurons into

a recurrent feedback network. Because the cells of this network obey membrane equations, the inhibitory interneurons within such a population of recurrent interactions tend to normalize their *total* activity across the entire interneuron population (Grossberg, 1973, 1980b). The total inhibition that converges on a target cell thus tends to be conserved as the total number of inputs varies, thereby preventing the problems stated above. If this property is experimentally confirmed, then it will be an interesting example of how less order on one level of biological organization generates more order on a higher level. In particular, the crucial self-normalization property can be achieved simply by allowing the inhibitory interneurons to randomly inhibit all cells within their range, rather than restricting their inhibition to excitatory target cells. As a result of this less ordered growth of inhibitory connections, the stability of the total network is facilitated.

Maintaining the balance between excitation and inhibition within the layer 6-to-4 on center does not imply that inhibition is weak. In fact, layer 4 cells that receive only off-surround inputs can be strongly inhibited. The model suggests below how the on-center off-surround network from layer 6-to-4 can use this property to selectively amplify the strongest perceptual groupings in layer 2/3 while using the off-surround to actively suppress LGN inputs to layer 4 that correspond to weaker groupings in layer 2/3. The weaker groupings hereby collapse. This is proposed to happen as follows.

Columnar Organization via Folded Feedback

Active model layer 4 cells are assumed to generate inputs to pyramidal cells in layer 2/3 via pre-developed pathways. These layer 2/3 cells initiate the formation of perceptual groupings via horizontal connections that self-organize during model development. How these horizontal connections develop in the model is described below. Before describing this, we first note what happens when layer 2/3 cells are activated. Throughout the developmental process, all cells that are activated in layer 2/3, whether by bottom-up or horizontal inputs, send excitatory feedback signals to layer 6 via layer 5 (Gilbert and Wiesel, 1979; Ferster and Lindström, 1985), as in Figure 1*b*. (The model does not attempt to discuss any other functional role for layer 5, notably its role in generating signals to motor control centers.) Layer 6, in turn, once again activates the on-center off-surround network from layer 6-to-4. This process is called *folded feedback* (Grossberg, 1999), because feedback signals from layer 2/3 get transmitted in a feedforward fashion back to layer 4. The feedback is hereby 'folded' back into the feedforward flow of bottom-up information within the laminar cortical circuits.

Folded feedback is predicted to be a mechanism that binds the cells throughout layers 2/3, 4, 5 and 6 into functional columns (Mountcastle, 1957; Hubel and Wiesel, 1962, 1977). The on-center off-surround network from layer 6-to-4 responds to its layer 2/3 inputs by helping to control which combinations of cells remain simultaneously active during development, and thus which cells will wire together, because 'cells that fire together wire together'.

In particular, early during the development of model horizontal connections in layer 2/3, the activation of layer 2/3 cells can cause horizontal activations that are relatively unselective for colinear position and orientation (Galuske and Singer, 1996; Ruthazer and Stryker, 1996). Without further selection among the possible activations, cortical interactions could remain both spatially and orientationally dispersed. This is corrected in the model via the intracortical folded feedback loop. In particular, suppose that a combination of bottom-up inputs and horizontal connections activates one subset of layer 2/3 cells a little more than a nearby subset of cells. Then, other things being equal, the favored layer 2/3 cells more vigorously activate their layer 2/3-to-5-to-6 pathway, and then their on-center off-surround layer 6-to-4 circuit. As a result, the cells whose activities form the strongest layer 2/3 grouping will suppress the activities of other cells via the layer 6-to-4 off-surround. The winning cells then get connected together via development, leading to a progressive increase in the projection range and orientational selectivity of these cells, as simulated in the Results section.

This refinement process exploits the fact that orientationally tuned simple cells in the model and the brain can bias development to favor long-range horizontal connections that are colinear with the preferred orientations of spatially aligned simple cells (Fitzpatrick, 1996; Schmidt *et al.*, 1997a). It is shown below how such oriented and colinear horizontal connections develop from an initial state in which no horizontal connections exist at all. It is also shown that, after development self-stabilizes, the same properties play a key role in generating perceptual groupings which exhibit properties of adult neurophysiological and psychophysical data.

Horizontal Connections and Perceptual Grouping

How these developing horizontal connections are prevented from generating run-away excitation and uncontrollable growth is one of the key properties of the model. A clue may be derived from properties of adult horizontal connections. In areas V1 and V2 of the adult, layer 2/3 pyramidal cells excite each other using monosynaptic long-range horizontal connections. They also inhibit each other using short-range disynaptic inhibitory connections that are activated by the excitatory horizontal connections (Hirsch and Gilbert, 1991; McGuire *et al.*, 1991) (see Fig. 1*c*). The excitatory connections, which span several hypercolumns (Gilbert and Wiesel, 1979, 1989), are hereby balanced by inhibitory connections, which span a single hypercolumn (Lund and Yoshioka, 1991). Thus, the excitatory connections within layer 2/3 have a broader spatial extent than the inhibitory off-surround connections from layer 6-to-4, which in turn have a broader spatial extent than the inhibitory interneurons in layer 2/3. These relative relationships are also simulated in the model. A range of numerical values could be chosen which obey these qualitative constraints without disrupting the model's key properties. In fact, in simulations of how the model performs perceptual grouping and attention, the excitatory connections within model layer 2/3 in cortical area V2 are chosen to be longer than those in cortical area V1, as is also true in anatomical data (Grossberg and Raizada, 2000).

We show below how both types of connections can develop to generate perceptual groupings 'inwardly' between two or more image contrasts that are aligned colinearly across space (von der Heydt *et al.*, 1984; Redies *et al.*, 1986; Peterhans and von der Heydt, 1989; Grosof *et al.*, 1993), but not 'outwardly' from a single image contrast (Hirsch and Gilbert, 1991; Knierim and van Essen, 1992; Cannon and Fullenkamp, 1993; Somers *et al.*, 1995; Stemmler *et al.*, 1995). This is called the *bipole* property (Grossberg and Mingolla, 1985). Illusory contours provide an excellent example of the bipole property: if a single image contrast could generate outward groupings, then our percepts would become crowded with webs of illusory contours spreading out from every feature in a scene. On the other hand, percepts of illusory contours between two or more colinear inducers are commonplace (Kanizsa, 1979, 1985).

We now describe how a balance between layer 2/3 excitation and inhibition develops that helps to stabilize cortical development and leads to the bipole property in the adult. We call layer 2/3 pyramidal cells that receive bottom-up input from layer 4 'supported' cells, and those that do not 'unsupported' cells. In the model, if an unsupported cell, or cell population, receives a sufficient amount of horizontal excitation, then it will be driven above its firing threshold. The cell population will then output horizontal excitation to itself as well as to other pyramidal cell populations. Unsupported cells can generate suprathreshold excitation if they receive enough horizontal excitation from supported cells. Turning off input support from layer 4 causes all supported cells, and then all layer 2/3 activities, to decay to zero. Therefore, boundaries can group across a gap provided the gap is small enough and the grouping signals from the supported cells on each end of the gap are sufficiently strong to drive the interior, unsupported cells above threshold.

The horizontal excitation from a single supported cell population cannot cause runaway excitation and outward grouping among unsupported cells because it also activates balanced disynaptic inhibition from smooth stellate cells. In this situation, the disynaptic inhibition is proportional to the horizontal excitation because both pyramidal and smooth stellate cells receive the same horizontal input signal. Given that horizontal excitation from a single supported cell population is inhibited by disynaptic inhibition, how do groupings ever span a region of unsupported cells? One factor is that inhibition from smooth stellate cells to pyramidal cells can lag behind the direct excitation between pyramidal cells due to the time it takes the smooth stellate cells to integrate their inputs. Therefore, synchronized inputs to layer 2/3 facilitate grouping because they allow the horizontal signals to summate at the target pyramidal cells before inhibition from local smooth stellate cells takes

effect. This property is consistent with the finding of Usher and Donnelly that visual groupings are facilitated when inducers are presented synchronously (Usher and Donnelly, 1998).

This argument about synchrony is not sufficient, however, to explain how inward grouping succeeds whereas outward grouping does not. The model notes that when two or more pyramidal cell populations are activated at positions that are located at opposite sides of an unsupported pyramidal cell, then excitation from these cells more easily summates at the unsupported cell, which can therefore exceed its firing threshold. In addition, this excitation activates the corresponding disynaptic inhibitory interneurons. As in the case of the layer 4 off-surround, the model disynaptic inhibitory interneurons are predicted to inhibit each other as well as the pyramidal cells. This model hypothesis is consistent with anatomical data showing that inhibitory layer 2/3 interneurons synapse on both pyramidal cells and other interneurons (McGuire *et al.*, 1991; Kisvarday *et al.*, 1993). Hence the total activation within such a population of inhibitory interneurons is predicted to be at least partially normalized. As a result, total activation may grow less quickly than summating activation of the pyramidal cells. The model hereby predicts that recurrent inhibition may influence the excitatory–inhibitory balance in both layer 2/3 and layer 4. In summary, due to a combination of spatial summation factors in the sources of excitation, and delays and amplitude properties of inhibition, net activation of the target pyramidal cells is possible, and grouping can occur inwardly but not outwardly, thereby realizing the bipole property (Grossberg and Mingolla, 1985), which has been used to explain and predict many perceptual grouping data (Born and Tootell, 1991; Shipley and Kellman, 1992; Watanabe and Cavanagh, 1992; Field *et al.*, 1993; Grossberg, 1994, 1997; Polat and Sagi, 1994; Gove *et al.*, 1995; Dresp and Grossberg, 1997; Grossberg and Pessoa, 1998).

There is more neurophysiological evidence for the bipole property in cortical area V2 (von der Heydt *et al.*, 1984; von der Heydt and Peterhans, 1989) than in V1. In V1, just a few unsupported cells have, to date, been found that show full activation of unsupported cells by pairs of supporting cells. More V1 cells show a modulatory influence from neighboring pyramidal cells (Redies *et al.*, 1986; von der Heydt and Peterhans, 1989; Grosof *et al.*, 1993; Kapadia *et al.*, 1995). These are challenging experiments to do in V1 because of the shorter horizontal connections there, and the existence of feedback from V2, which has longer horizontal connections. Unsupported V2 cells could be fully activated by stimuli that fall outside the V1 receptive fields, and could modulate V1 cells by top-down feedback. For simplicity, the present model assumes that the bipole property holds in both V1 and V2. Altering the model to allow only modulatory bipole influences in V1 can be accomplished by changing the model parameters that control whether convergent horizontal connections can fire the cell in the absence of bottom-up input; see the Appendix, equations (26)-(28).

Developmental Growth Rules

These properties of adult grouping arise in the model by specializing two well-known developmental rules. The first rule is that axons are attracted to cell targets when the source and target cells are both active (Gunderson and Barrett, 1979, 1980; Letourneau, 1978; Purves and Lichtman, 1980; Lichtman and Purves, 1981). The second rule is that axons compete intracellularly for growth resources (Purves and Lichtman, 1980; Lichtman and Purves, 1981). In the present instance, the first rule enables horizontal connections to form if activations in a source pyramidal cell and a target pyramidal cell are sufficiently correlated — in particular, if the target cell satisfies the bipole property — and removed if they are not (Callaway and Katz, 1990, 1991; Lowel and Singer, 1992). This rule is realized by an activity-dependent morphogenetic gradient whose strength decreases with distance from the target cell that emits it. The gradient influences horizontal growth only in active source cells. As contact between two cells is achieved, a synaptic learning law strengthens the synaptic contact by continuing to sense the correlation between presynaptic and postsynaptic activity.

The second rule prevents uncontrolled proliferation of horizontal connections by withdrawing connections from target cells that are receiving more poorly correlated signals than other target cells. The two rules work together to withdraw connections from cells that may be activated by weakly correlated image features or statistically insignificant noise. These model mechanisms for axonal growth and synaptic tuning *dynamically* stabilize cortical development as the developing cortical structure matches the statistics of its environmental inputs. If this match is disrupted later in life, then a new bout of development and/or learning can be triggered by the same mechanisms. Because of this property, the model can be used to clarify data about shared molecular substrates of neonatal development and adult learning (Bailey *et al.*, 1992; Kandel and O'Dell, 1992; Mayford *et al.*, 1992), plasticity of adult cortical representations after lesions (Merzenich *et al.*, 1988; Chino *et al.*, 1992; Gilbert and Wiesel, 1992; Darian-Smith and Gilbert, 1994; Kapadia *et al.*, 1994; Das and Gilbert, 1995; Schmidt *et al.*, 1996), dynamical reorganization of long-range connections in the visual cortex (Gilbert and Wiesel, 1992; Zohary *et al.*, 1994), and perceptual learning in the adult (Karni and Sagi, 1991; Poggio *et al.*, 1992). In fact the model equations for activity-dependent control of synaptic strength have already been used to explain properties of adult learning (Grossberg, 1980a; Carpenter and Grossberg, 1991).

Top-down Feedback from V1 to LGN

Layer 6 of model area V1 sends top-down feedback to the LGN via an on-center off-surround network, as also occurs *in vivo* (Murphy and Sillito, 1987; Weber *et al.*, 1989; Murphy and Sillito, 1996) (see Fig. 1*d*). The feedback on-center reinforces the activities of those LGN cells which have succeeded in activating V1 cells, notably V1 cells whose activations represent the strongest perceptual groupings. The feedback off-surround suppresses the activities of other LGN cells. As in the brain, this model feedback circuit increases the useful visual information that is transmitted from LGN to cortex by enhancing contextually significant differences between LGN responses (McClurkin *et al.*, 1994), and also influences the length tuning of LGN cells (Murphy and Sillito, 1987). The LGN to V1 circuit is also known to be modulatory (Sillito *et al.*, 1994). Earlier modeling work predicted that this feedback pathway plays a role in stabilizing the development of bottom-up connections from LGN to V1, as well as the reciprocal top-down connections from V1 to LGN (Grossberg, 1976b, 1980b). Grunewald and Grossberg have modeled how the normal development of bottom-up disparity tuning can occur at V1 complex cells when such top-down feedback is operative, and have shown how this development may break down when it is not (Grunewald and Grossberg, 1998). Further experimental study of this question is needed. For purposes of the present modeling analysis, it is assumed that these top-down connections are pre-developed and are available to facilitate activation of the correct combinations of simple and complex cells.

Results

Developmental Data and Simulations

The next three sections summarize how the model simulates data about the development of long-range horizontal connections in area V1. After development self-stabilizes, the resultant network can, without further change, simulate adult neurophysiological and psychophysical data. As in the brain, the model undergoes two stages of development (Fig. 2). One occurs prior to eye opening, when endogenous random geniculate and cortical activity determine the initial specificity of horizontal connections (Ruthazer and Stryker, 1996). The other occurs after eye opening, when patterned visual inputs can strengthen and refine these connections (Galuske and Singer, 1996).

Several anatomical studies have investigated how horizontal projections develop in the superficial layers of visual cortex into adult connections that connect columns of similar orientation preference (Callaway and Katz, 1990; Durack and Katz, 1996; Galuske and Singer, 1996). Callaway and Katz used neuronal tracing and intracellular staining to investigate the development of clustered horizontal connections in cat striate cortex (Callaway and Katz, 1990). They found an even, unclustered distribution up to 2 mm from the injection site during the first

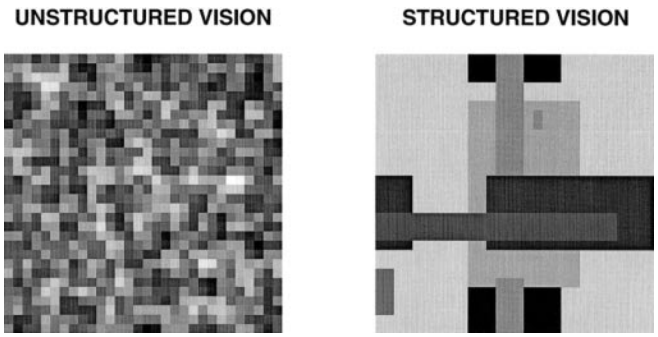

Figure 2. Example training image, consisting of Gaussian filtered random noise, used to model unstructured vision prior to eye opening. Right: example training image, consisting of seven randomly configured rectangles, with input values randomly distributed between 0 and 2, used to model structured vision after eye opening.

postnatal week, followed by an increase in the range and clustering of the projections in the second postnatal week, when the eyes are opened, and finally a long, slow refinement of projections due to the elimination of some connections until an adult level of clustering was reached in the sixth postnatal week.

Increase of Projection Range

The Galuske and Singer investigation of long-range projections in cat area 17 (the analog of monkey area V1) at different stages of postnatal development yielded a similar conclusion (Galuske and Singer, 1996). These authors also reported quantitative data about the projection range of pyramidal cells (Fig. 3, top). Soon after eye opening, the projection range doubled over a period of 12 days (from P15 to P26). Presumably, the increase in projection range is due to the greater correlations in activity over large spatial distances that occurs in natural, structured images. Figure 3 (bottom) shows the simulated projection range in the model. Before eye opening, the short-range spatial correlations of the unstructured inputs are reflected in the relatively short-range extent of horizontal projections. Soon after eye opening, the long-range spatial correlations in the structured visual inputs cause the projection range to double, just as in the data of Galuske and Singer (Galuske and Singer, 1996). These results exploit the developmental rules described above by causing a larger projection range to grow when the statistics of visual imagery provided more long-range correlations.

Increase of Orientational Selectivity

A similar pattern of exuberant growth followed by slow refinement of projections has also been found in the ferret. Because the ferret is born 3 weeks earlier in development than the cat, it has more stable orientation-selective cortical cell responses than the cat during the period in question (Durack and Katz, 1996; Ruthazer and Stryker, 1996). Ruthazer and Stryker reported quantitative data about the growing orientational selectivity of horizontal clustering over time, using a statistic called the cluster index (CI) (Ruthazer and Stryker, 1996). The CI measures the log of the average nearest-neighbor distance between horizontal projections within a measurement window, divided by the average distance between a randomly selected point in the window and the nearest horizontal projection. Therefore, a uniform distribution of horizontal projections would lead to a CI of log(1) = 0. As clustering becomes more refined, CI increases. Figure 4 (top) shows the CI obtained by Ruthazer and Stryker from 21 days postnatal up to adult age (Ruthazer and Stryker, 1996). Before eye opening, which is

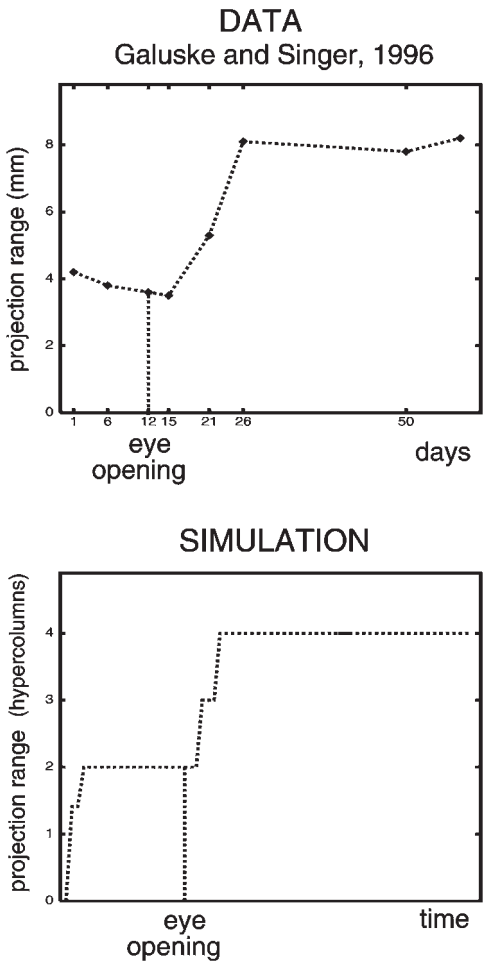

Figure 3. Top: projection range of pyramidal cells in cat visual cortex as a function of age. Projection range doubles after eye opening. [Adapted from Galuske and Singer (1996).] Bottom: projection range of model pyramidal cells during development. Model projection range also doubles after 'eye opening'.

about 31 days postnatal, there is a positive CI, indicating a clustering bias, presumably favoring iso-orientation connections. After eye opening, the CI rapidly increases to reflect the strong, adult bias in favor of iso-orientation connections.

The model does not represent individual horizontal projections, but rather the average strength of horizontal projections from an orientation column to other orientation columns. Therefore, the model's format is unsuitable for computing a CI index. An analogous measurement of orientation preference was computed by dividing the strength of a column's horizontal connections to nearby columns with the same orientation preference by the strength of all the column's horizontal connections. This statistic is shown in Figure 4 (bottom). Like the CI index, it shows an initial moderate bias in favor of iso-orientation connections that dramatically increases after eye opening. In order to make the computer simulations tractable, the model presently represents only two orientations (vertical and horizontal) so Figure 4 shows the bias in favor of one orientation over the perpendicular orientation. If the model represented intermediate orientations as well, then the relative iso-orientation bias would be smaller because the presence of intermediate orientations would reduce the average orientation distance between iso- and non-iso-orientation columns.

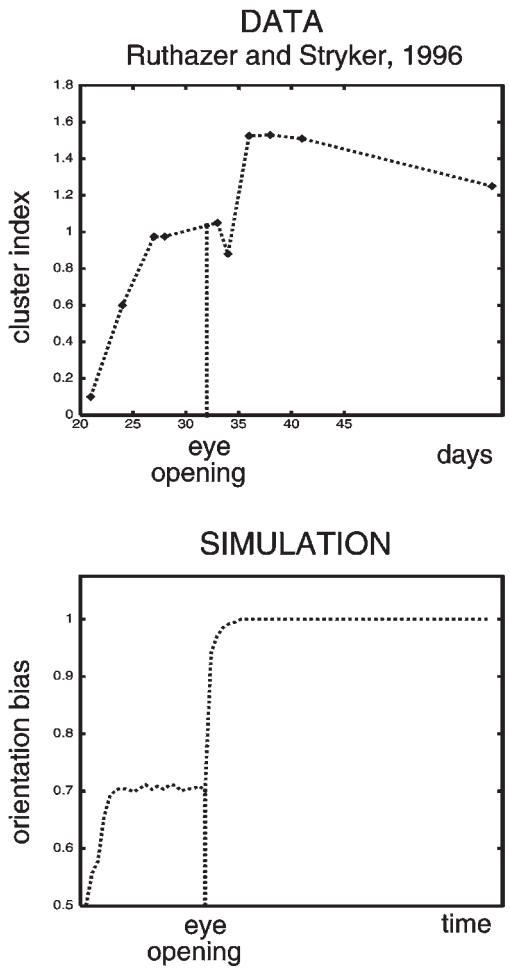

Figure 4. Top: mean cluster index (CI) in ferret area 17 as a function of age (from Ruthazer and Stryker, 1996): 'At P27 horizontal connections are significantly clustered, but single-unit recordings reveal poor orientation selectivity (25% of cells have orientation-selective responses), and optical imaging does not yet show an orientation map. Between P32 and P36, a secondary refinement of horizontal connections occurs along with the maturation of single-unit orientation selectivity and the emergence of the earliest optical orientation maps.' Eye opening takes place at about P31. [Adapted from Ruthazer and Stryker (1996).] Bottom: clustering bias in model during development. The strength of horizontal connections to iso-orientation columns divided by the net strength of horizontal connections is plotted as a function of age. Like the data of Ruthazer and Stryker, the clustering bias increases after eye opening.

After development, horizontal projections preferentially connect columns with similar orientation preferences that are aligned colinearly with their orientation preference (Fitzpatrick, 1996; Schmidt *et al.*, 1997a). Figure 5 (left) shows a polar plot by Fitzpatrick of the projection field from a site in layer 2/3 of tree shrew striate cortex (Fitzpatrick, 1996). The distance of each point from the center of the projection field represents the number of labeled terminals at that angle (in 10° increments). The orientation of the projection field is aligned with the orientation preference of its source neuron. Figure 5 (right) shows the analogous projection field from a horizontally tuned column in layer 2/3 of the model after development has equilibrated. The size of each circle represents the strength of the connection to each iso-orientation column. The anisotropy of the model's projection field is qualitatively consistent with Fitzpatrick's data. These results derive from the fact that visual cues are, with high probability, locally linear across space, so

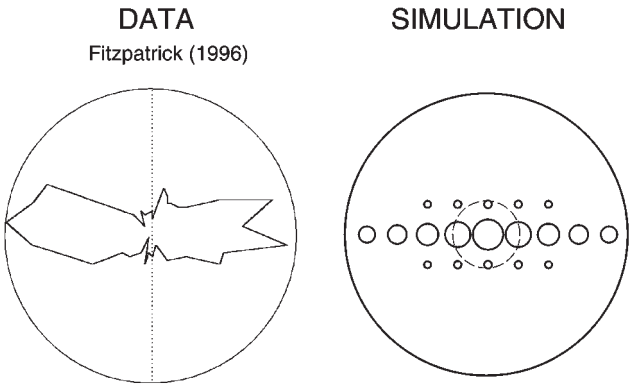

Figure 5. Left: polar plot of the projection field from a site in layer 2/3 of tree shrew striate cortex. The orientation of the projection field is in agreement with the orientation preference of its source neuron. [Adapted from Fig. 11 of Fitzpatrick (1996)]. Right: the projection field from a horizontally tuned column in layer 2/3 of the model after learning has equilibrated. The size of each circle represents the strength of the connection to each iso-orientation column. The dashed circle in the middle shows a layer 2/3 cell's classical receptive field, which is the spatial extent within which a point input causes the cell to 'fire' (i.e. go above its output threshold).

that the largest correlations would be generated by cells whose orientations match those of the input and are colinearly aligned across space. The developmental rules enable the network to sense these correlations and to selectively amplify the growth of those connections which best match them.

Neurophysiological Data and Simulations

Projection Field versus Receptive Field

This section shows that the model network that develops has neurophysiological properties that have been recorded from adult animals. One such property shows, remarkably, that the extent of a cell's total anatomical projection field is much greater than that of its classically recorded receptive field (Fitzpatrick, 1996). Fitzpatrick found that the projection fields in tree shrew extend for >2 mm from the injection site, a distance that corresponds to 15° eccentricity, whereas the dimensions of classically defined receptive fields at that eccentricity are <5°. The dwarfing of classical receptive fields by projection fields was also shown in neurophysiological data recorded from cats by Das and Gilbert (Das and Gilbert, 1995). These authors compared cortical point spread (PS) distributions, measured with optical recording, which reflect both spiking and subthreshold activity, with spiking distributions measured with extracellular electrodes. A small oriented visual stimulus produced a PS distribution 20 times larger than the spiking distribution. Moreover, the close match of the PS distribution with columns whose orientation preference agrees with the orientation of the visual stimulus suggests that the distribution arises from iso-oriented long-range horizontal projections.

A similar property holds in the model after development equilibrates: Figure 5 (right) shows the size of a layer 2/3 cell classical receptive field (dashed-line circle) with respect to its projection field in the model. This discrepancy between projection field and receptive field can be traced to the model's bipole property: the classical receptive field reflects mainly bottom-up properties of the cortical network in the model, whereas the subthreshold activations reflect the fact that the bipole requirement for firing the cells via long-range horizontal connections was not satisfied.

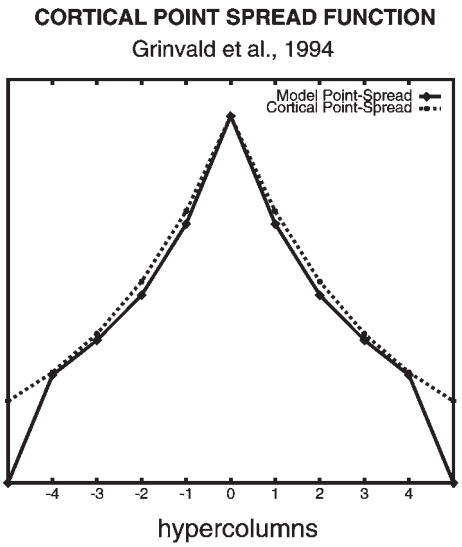

Figure 6. Comparison of cortical point spread function modeled by Grinvald *et al.* (1994) based on optical recordings in macaque primary visual cortex, with analogous point spread function produced by our developed model. A close match is obtained out to four hypercolumns away from the source cell, which is the maximal extent of model horizontal projections. The point spread function of Grinvald *et al.* (1994) is an exponential decay function with a space constant of 1.5 mm. (if ocular dominance columns of only one eye are considered). This function was converted to the model's metric of cortical columns by assuming that iso-orientation columns are spaced 450 mm apart.

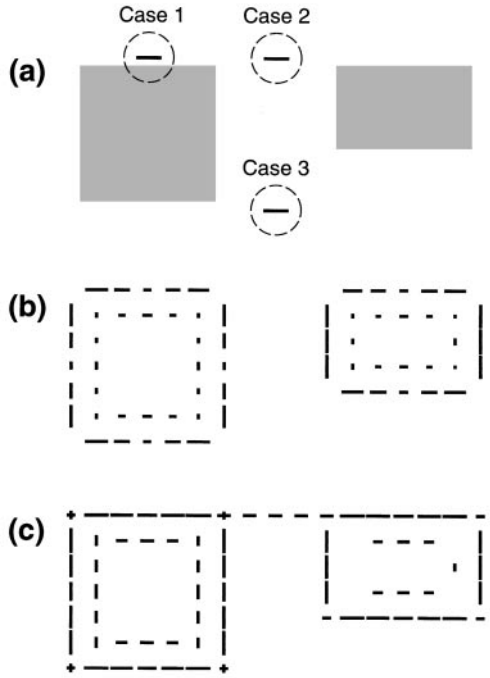

Figure 7. (*a*) Input image consisting of a 5 × 5 pixel square and a 5 × 3 pixel rectangle, separated by a 5-pixel gap. (*b*) Equilibrated suprathreshold activities of model layer 4 cells. (*c*) equilibrated suprathreshold activities of model layer 2/3 cells. See text for details.

Cortical Point Spread Functions

The measurement of cortical point spread functions (PSFs) provides additional evidence about the strength of horizontal connections. In this regard, optically recorded signals are believed to arise from subthreshold dendritic activity in the superficial layers (Grinvald *et al.*, 1994). These dendrites may belong to cells in both the superficial and deep layers. Grinvald *et al.* measured an asymmetric PSF in macaque monkeys, with twice as much spread along the axis parallel to the V1/V2 border as along the perpendicular axis (Grinvald *et al.*, 1994). The axis parallel to the V1/V2 border is perpendicular to the direction of OD columns in this cortical region. Therefore, the explanation given by Grinvald *et al.* for this asymmetry is that a spread in activity among the equivalent number of same-eye OD columns would traverse twice as much cortical surface in the axis perpendicular to the direction of OD columns. Accordingly, they modeled the PSF with an asymmetric two-dimensional exponential distribution, having a space constant of 3.0 mm in the axis perpendicular to OD columns, and 1.5 mm in the axis parallel to OD columns.

In comparing the PSF obtained by our model with this experimentally derived distribution, it is appropriate to use the 1.5 mm space constant because our model is monocular. The only remaining step is to map the metric of cortical surface distance into the metric of model hypercolumns. We found the best-fitting match by assuming that a hypercolumn in our model would have a diameter of 450 μm parallel to the direction of OD columns, and therefore 900 μm perpendicular to the direction of OD columns. Given this assumption, Figure 6 compares the experimentally derived PSF with the PSF generated by our model following stimulation in the center hypercolumn. These PSFs closely resemble each other out to four hypercolumns away from the central one.

The PSF produced by the model is based on the assumption that the point spread consists solely of activity in layer 2/3 apical dendrites. In the model, these dendrites are excited by the layer 2/3 horizontal projections. Therefore the PSF plotted in Figure 6 equals the spatial distribution of the strengths of horizontal signals from the central orientation column to nearby iso-orientation columns. The model PSF matches the exponential distribution out to four hypercolumns because model parameters were set, for computational tractability, to prevent its horizontal projections from growing beyond this extent.

Psychophysical Data and Simulations

After model cortical development stabilizes, the cortical network that is formed in this way, without further change, simulates key psychophysical data about adult perceptual grouping. Facilitation of cortical responses by oriented, colinearly arrayed inducers has been found by a number of researchers (von der Heydt *et al.*, 1984; von der Heydt and Peterhans, 1989; Field *et al.*, 1993; Grosof *et al.*, 1993; Polat and Sagi, 1993, 1994; Kapadia *et al.*, 1995). Many of these facilitory effects may be explained by colinear groupings mediated by layer 2/3 connections in V1 and V2, or by groupings that form perpendicular to line ends. That is why the current self-organized model was restricted to horizontal and vertical orientations, and was used to study how grouping strength changed when the spatial separation of inducers was varied.

Illusory Contour Formation

Figure 7 illustrates the model's grouping behavior. Figure 7*a* shows an input image consisting of a 5 × 5 pixel square and a 5 × 3 pixel rectangle, separated by a 5-pixel gap. Figure 7*b*,*c* shows the network's equilibrated suprathreshold layer 4 and layer 2/3 activities, respectively, in response to this image. In these

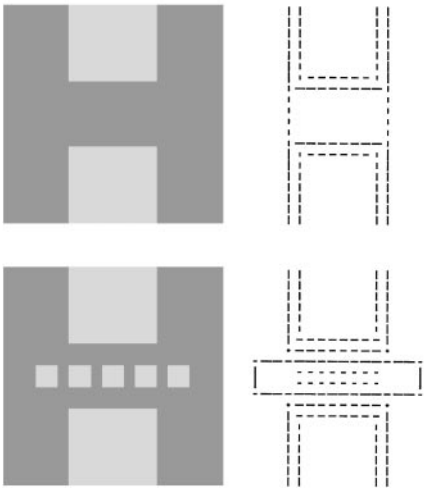

Figure 8. Top: (Left) Two aligned vertical bars (8 pixels wide) separated by 6-pixel gap. (Right) Equilibrated suprathreshold activities of model layer 2/3 cells, showing vertical grouping of bars. Bottom: (Left) Same two vertical bars, with five 2-pixel-wide squares aligned horizontally in the gap. (Right) Equilibrated suprathreshold activities of model layer 2/3 cells, showing that horizontal grouping of the squares blocks the vertical grouping of the bars.

line-segment displays, the orientation of each boundary segment denotes the orientation preference of the cell at that location, and the length of the segment denotes the cell's activity.

The layer 4 excitatory cells (Fig. 7*b*) detect the location and orientation of the object edges: case 1 in Figure 7*a*. These cells respond more strongly near the object corners due to end-stopping caused by layer 6-to-4 inhibition. Layer 4 cells input to layer 2/3 excitatory cells, whose activations (Fig. 7*c*) code object boundaries as well as boundary grouping between the objects. The tops of the two objects are grouped together by the layer 2/3 horizontal interactions (case 2 in Fig. 7*a*) because they are colinear with each other and because the gap separating them is sufficiently small. The non-colinear lower edges of the object (case 3 in Fig. 7*a*) do not group, even though they are both horizontally oriented. Such a grouping 'inwardly' between two or more like-oriented and colinear image contrasts, but not 'outwardly' in response to a single contrast, illustrates that the bipole property is realized at the layer 2/3 model cells after development of the horizontal and interlaminar interactions.

Contour Sensitivity to Spatial Context

The model's context-sensitivity also includes the property of spatial impenetrability (Grossberg and Mingolla, 1987), in which boundary groupings in one orientation inhibit weaker potential groupings in other orientations at the same position. Figure 8 illustrates this property. Figure 8 (top left) shows two aligned vertical bar inputs, and Figure 8 (top right) shows how the network's equilibrated suprathreshold layer 2/3 pyramidal cell activities vertically group the two bars together. Figure 8 (bottom left) shows a modified input with same two bars augmented by several squares aligned horizontally in the gap between them. These squares do not individually favor horizontal over vertical grouping. In fact, the vertical sides of two of the squares are colinear with the vertical sides of the bars. Other things being equal, they would facilitate vertical grouping. On the other hand, the set of all the squares, taken together, generates a strong horizontal grouping. The emergent horizontal orientation of this grouping inhibits the vertical grouping, as

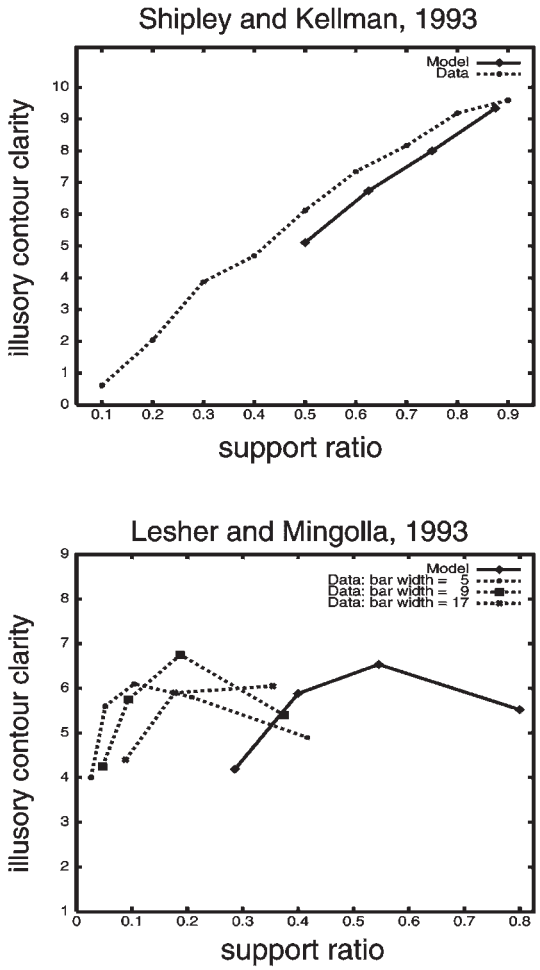

Figure 9. Top: Shipley and Kellman (1993) obtained clarity ratings for illusory contours as a function of their support ratio. The stimulus was a 4 cm illusory Kanizsa square, induced by four Pacmen figures. As the support ratio increased (i.e. the size of the Pacmen increases and the size of the gap decreases) the illusory contour clarity increased roughly linearly. [Adapted from Fig. 5 of Shipley and Kellman (1993).] The model results were obtained by measuring the strength of vertical grouping between two aligned rectangles (3 pixels wide). The length of the rectangles plus gap was 8 pixels. As the size of the gap was decreased from 4 pixels to 1 pixel by increasing the length of the rectangles, the average grouping strength in the gap increased. See text for a description of how the grouping strength was mapped into a metric of perceived illusory contour clarity. Bottom: Lesher and Mingolla (1993) also obtained clarity ratings for illusory contours as a function of support ratio. However, they increased support ratio by increasing the number, and hence the density, of perpendicular bar inducers within concentric-ring Pacman stimuli that induce a percept of an illusory square. As the number of bars, and hence the support ratio, increases, the illusory contour clarity increases and then decreases. [Adapted from Figs 8*a* and 10*c* of Lesher and Mingolla (1993).] The model's illusory contour strength was measured along a 4-pixel gap. Inducers were 2-pixel-wide bars, with the spacing between bars varied to yield 1, 2, 3 and 4 bars on each side of the gap, with inter-bar spacing of 3, 2, 1 and 0 pixels, respectively.

shown in the equilibrated suprathreshold layer 2/3 pyramidal cell activities (bottom right). The network's spatial impenetrability is due to the cross-orientational inhibition that develops in layer 2/3 and layer 4. This simulation shows that the self-organized balance between the layer 2/3 horizontal excitation and disynaptic inhibition that achieves the bipole property is also well-balanced against the interlaminar 6-to-4 connections that help to select which groupings will survive.

Evidence for spatial impenetrability has been found in psychophysical and physiological experiments. Kapadia *et al.*

found that the detection threshold reduction that was caused by colinear facilitation between two aligned bars was inhibited by an interpolated perpendicular bar (Kapadia *et al.*, 1995). They found that this configuration abolished the enhancement of V1 cell firing caused by the colinear facilitation. Von der Heydt *et al.* found that the response of V2 cells in the gap between two aligned bars, which is believed to signal the presence of illusory contours in the gap, was abolished when thin, perpendicular bars were placed between the inducing bars and the gap (von der Heydt *et al.*, 1984).

It should be noted that the simulations describing perceptual grouping consider interactions within the interblob stream of visual cortex, which has been predicted to support such grouping dynamics (Grossberg and Mingolla, 1985). In fact, there is neurophysiological evidence that locally aligned contours can produce illusory contour-like responses in area V2 (Peterhans and von der Heydt, 1989). Grouping strength does not, however, necessarily covary with visibility, as measured, say, by a brightness or color difference. In fact, it has been predicted that the perceptual groupings which are formed in the interblob stream are *amodal*, i.e. they themselves do not represent a visible brightness or color signal. Visible brightness or color signals have been predicted to occur within the blob cortical stream as part of the process whereby three-dimensional surface representations are formed (Grossberg, 1994).

Contour Sensitivity to Support Ratio

Figure 9 shows how the illusory contours formed by the model, either colinear to edges or perpendicular to line ends, vary in strength as the inducing features are parametrically varied. These simulations illustrate that the developed layer 2/3 connections do not saturate; instead, they enable the network to exhibit the type of spatial context-sensitivity found in human psychophysical data. Figure 9 (top) plots data of Shipley and Kellman (Shipley and Kellman, 1992) which show the effect of increasing the length of the inducers while decreasing the gap between them, keeping the total length of inducers-plus-gap constant: illusory contour clarity increases roughly linearly. In other words, contour clarity increases with 'support ratio'. Figure 9 (top) shows that the clarity of the model's illusory contours also increases linearly as the support ratio is increased. The mapping from network activities to clarity ratings is described below. This result is due to the fact that, as the gap between two inducers is made smaller, the grouping signal becomes stronger, due to the monotonically increasing magnitude of the layer 2/3 grouping kernel towards its center (see Figs 5 and 6).

The model matches the psychophysical data well, with the caveat that the model cannot form illusory contours when the support ratio falls below 0.5. This is due to simplifications in the model — made for computational tractability — which limit the extent of the groupings it can make. In particular, model parameters were chosen so that its developed horizontal projections extend only four hypercolumns away from the center. In addition, the model only simulates grouping in V1 and does not take advantage of larger-scale processing in V2. Finally, the model does not include the retina-to-cortex cortical magnification factor (van Essen *et al.*, 1984), whereby scale expansion takes place as stimuli move into the periphery.

Figure 9 (bottom) summarizes psychophysical data obtained by Lesher and Mingolla showing that, if support ratio is increased in a different way, then an inverted-U in illusory contour clarity strength is obtained (Lesher and Mingolla, 1993). In this study, parallel bars with aligned ends were used to form four Pacman figures with which to induce an illusory Kanizsa square percept. The square formed perpendicular to the bars through their aligned ends. Contour clarity of the illusory square was measured as the numbers of bars, and hence the support ratio, varied. The inducing Pacmen had a circular radius of 128 pixels, and the gap between Pacman pairs in which the Kanizsa square percept formed was 128 pixels. The support ratio was computed as the number of bar inducers (1, 2, 4, 8, 16 per Pacman) times bar width, divided by the length of the side of the square (384 pixels). As the width of the bar inducers is increased, the number of possible inducers becomes limited, which is why there are only results for up to 16 inducers in the 9-pixel-wide case, and up to 8 inducers in the 17-pixel-wide case. Figure 9 (bottom) shows that the model simulates the inverted-U in contour strength as a function of bar density. This inverted-U result is due to an interaction between the long-range excitatory horizontal connections in layer 2/3 and the medium-range inhibitory connections from layer 6-to-4. The Shipley and Kellman data (Shipley and Kellman, 1992), and our simulation thereof, show that decreasing the distance between inducers, up to a certain point, increases grouping strength as a result of layer 2/3 horizontal cooperation. As the inducers get even closer together, however, layer 6-to-4 inhibition increasingly inhibits the net excitation caused at layer 4 by each LGN input. Thus, although more inputs activate the cooperating layer 2/3 pyramidal cells, the net effect of each input on layer 2/3 gets smaller as the inducers get denser. This simulation shows that the self-organized connections preserve a good balance between layers 6, 4 and 2/3. As in the psychophysical data in Figure 9, the model's illusory contour strength is affected more strongly by variations in support ratio than in bar density.

Due to the implementational limitations of the model described above, the network simulated these data using bars that are relatively wide with respect to the length of the gap (2-pixel-wide bars, 4-pixel -ong gap). Figure 9 (bottom) shows results obtained by the model with inter-bar gap size decreasing from 3 to 0, with the total length spanned by the inducers and gaps held roughly constant. The model's inverted-U curve is shifted to the right of the data curves, reflecting the fact that the model used inducers that were wider relative to the gap size. Note that, in the data as well, the curves shift to the right as the width of the inducers increases. Using short bars instead of line ends to simulate this result, due to limitations of cell density in the model, does not and should not alter the qualitative results because the model predicts that they are due to an interaction between how the bottom-up layer 6-to-4 off-surround attenuates the activation of layer 4 cells in response to bottom-up inputs before layer 4 cells can activate a horizontal grouping in layer 2/3, in response to *any* input pattern, as its inducers get closer together.

Mapping Network Activity into Illusory Contour Clarity

The model's layer 2/3 activities were mapped into the psychophysical illusory contour clarity metric (ICC) via the following equation:

$$\mathrm{ICC} = \rho(C_{\max} - C_{\min})\bar{z} + C_{\min} \qquad (1)$$

where ρ is a scaling parameter, $C_{\max}$ and $C_{\min}$ are the maximum and minimum of the clarity scale, and $\bar{z}$ is the average amount of suprathreshold activity in layer 2/3 excitatory cells along the gap:

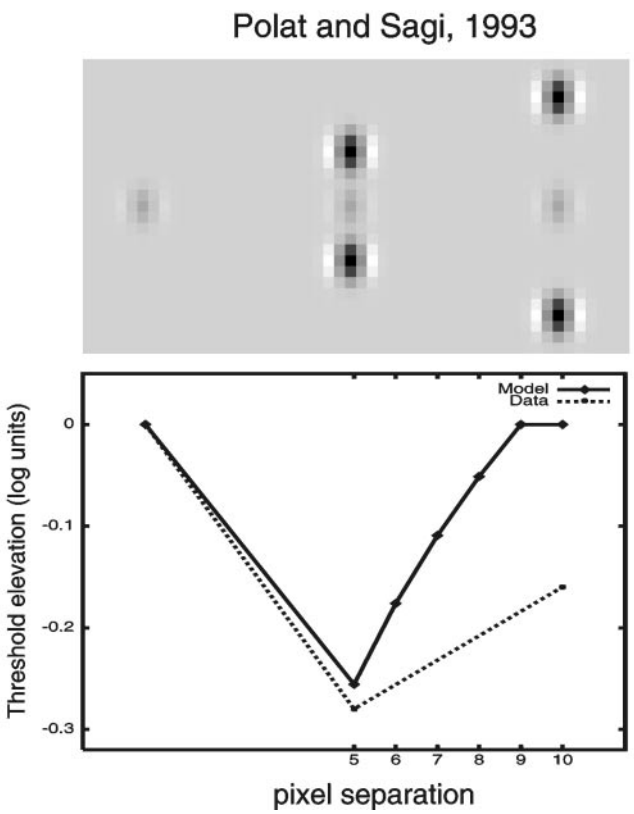

Figure 10. Bandpass-limited inducers (Gabor patches). As the spatial separation of the flanking patches was increased (middle and right), the detection threshold for the central patch decreased and then slowly increased back to the baseline threshold obtained for the central patch alone (left). [Adapted from Figure 2 of Polat and Sagi (1993).] The model obtained the same qualitative results. The model's detection threshold is plotted as a function of the separation (between patch centers) of the flanking stimuli. The baseline detection threshold was calculated as the amplitude coefficient for the central Gabor patch which caused the the average layer 2/3 activation level (within a 5 × 5 pixel window centered on the Gabor patch) to reach 0.05. This corresponds roughly to having a majority of layer 2/3 cells within the patch go above their firing threshold.

$$\bar{z} = \frac{\sum_{ij \in \text{gap}} \left[z_{ij} - \Gamma \right]^{+}}{\sum_{ij \in \text{gap}} 1} \qquad (2)$$

Model fits to both data sets used ρ = 0.85.

Detection Threshold Context Sensitivity

Figure 10 (top) shows bandpass-limited inducers (Gabor patches) similar to those used by Polat and Sagi in their psychophysical experiments (Polat and Sagi, 1993). If the spatial separation of the flanking patches is sufficiently small that the patches overlap, then the threshold for detecting the target Garbor patch is greater than the baseline threshold for the target patch alone. This threshold increase is due to mutual inhibition between representations of the nearby stimuli and/or a reduction in the signal to-noise ratio for the central stimulus. If the separation is increased such that the patches do not overlap, then the detection threshold decreases below the baseline threshold. As the separation is further increased, the detection threshold gradually returns to the baseline level. Figure 10 shows an optimal separation that yielded a reduced threshold (middle) in Polat and Sagi's experiments, and a larger separation for which this reduction was diminished (right).

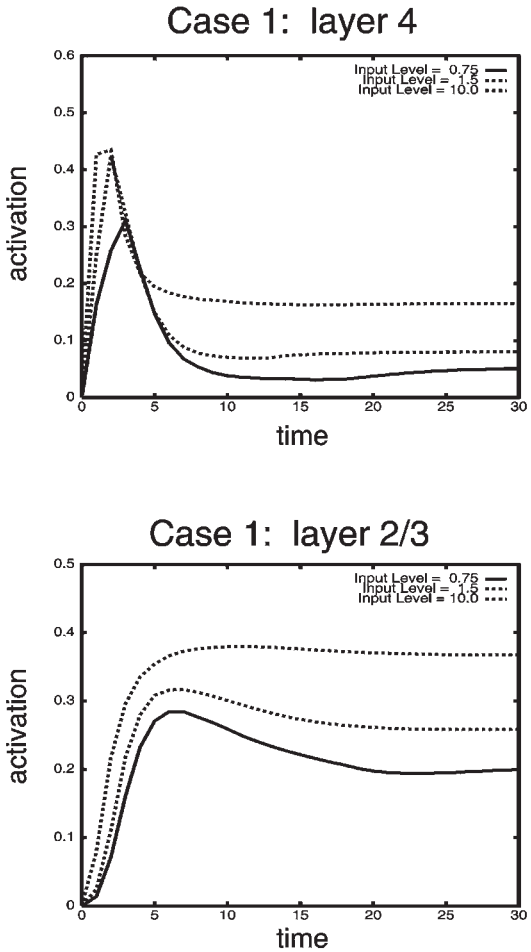

Figure 11. Top: layer 4 cell activity as a function of time in case 1 of Figure 7 for three different input levels. Bottom: layer 2/3 cell activity.

We simulated the cases in which the Gabor patches do not overlap to avoid the complications involved in measuring the detection of a signal (the target Gabor patch) in the presence of noise (the overlapping Gabor patches). With this proviso, the model obtains similar results to those found by Polat and Sagi (Polat and Sagi, 1993). Figure 10 (bottom) plots the detection threshold as a function of the separation (between patch centers) of nonoverlapping flanking stimuli. The largest threshold reduction is obtained with a 5-pixel separation (middle). Increasing this separation reduces the effect until, at a 9-pixel separation, the baseline threshold is obtained. The discrepancy between the model's results and psychophysical data at large separations is due to the model simplifications described above.

Contrast-sensitive Temporal Dynamics of Perceptual Grouping

Using the input stimuli of Figure 7*a*, the contrast-sensitive temporal dynamics underlying grouping were analyzed by examining the activities over time of horizontally oriented layer 4 and layer 2/3 cells whose receptive fields are placed: along an object contour (case 1), in the middle of a gap between two colinear contours (case 2), and the same distance from a single colinear contour (case 3).

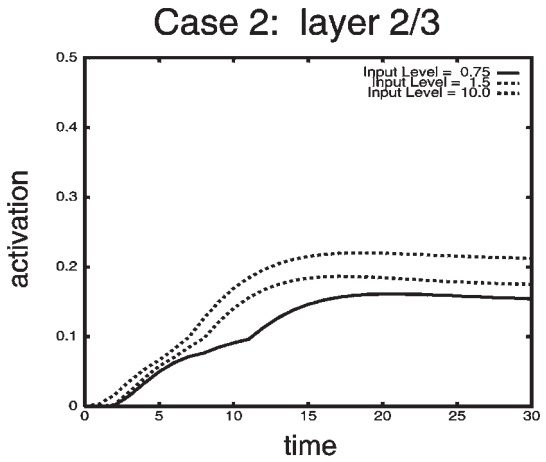

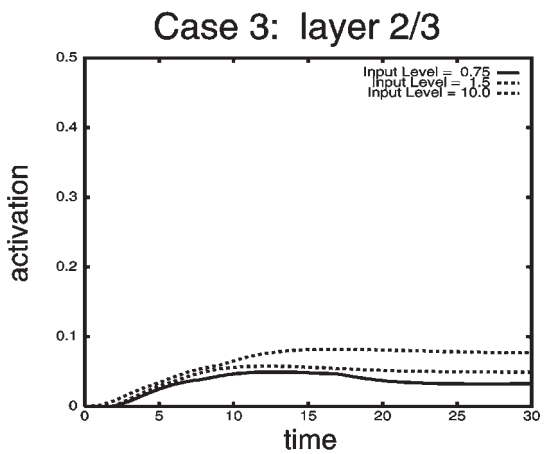

Figure 12. Top: layer 2/3 cell activity as a function of time in case 2 of Figure 7 for three different input levels. Bottom: layer 2/3 cell activity in Case 3.

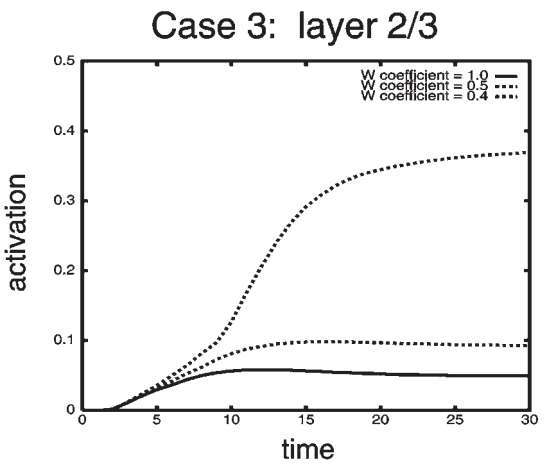

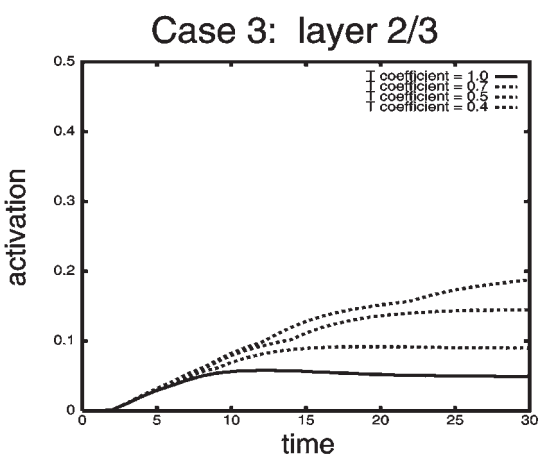

Figure 13. Top: layer 2/3 cell activity in case 3 of Figure 7 with normal W^+ kernel, and with W^+ kernel reduced by 40 and 50%. Bottom: layer 2/3 cell activity in case 3 of Figure 7 with normal T^+ kernel, and with T^+ kernel reduced by 30, 40 and 50%. See text for details.

Figure 11 (top) plots a layer 4 cell's activation as a function of time in case 1 for three different input levels I_{ij} in equations (1) and (2). The cell has an initial burst of activity which is largely attenuated by subsequent inhibition from layer 4 interneurons, which are activated from layer 6. As the input increases, the layer 4 activity peaks earlier, and equilibrates at a higher level. Figure 11 (bottom) plots the activation of the corresponding layer 2/3 cell. The layer 2/3 activity also peaks earlier, and equilibrates at a higher level.

Next we look at what happens in the two types of gaps, a gap that is surrounded by two colinear edges (case 2), and a gap that is next to only one edge (case 3). In both of these cases, the layer 4 cell remains inactive because there is no bottom-up input at the position of the gap measurement. We therefore plot only the layer 2/3 cell's activation, which is determined solely by horizontal input from other layer 2/3 cells. In Figure 12 (top), the layer 2/3 cell's activity stabilizes above the output threshold (Γ = 0.1) for all three contrast levels, so that an illusory contour is formed between the two colinear gaps. The input contrast once again determines both the rise time and the final level of the cell's activity.

In Figure 12 (bottom), on the other hand, the layer 2/3 cell activation stabilizes below the output threshold of 0.1 for all three contrast levels. Here, the layer 2/3 cell receives horizontal input only from layer 2/3 cells on one side. Thus, Figure 12 shows that the bipole grouping rule is realized for a wide range of input contrast levels.

Destabilization of Perceptual Grouping by Unbalanced Excitation and Inhibition

The bipole rule requires that layer 2/3 cells remain subthreshold, as in Figure 12 (bottom), unless they are surrounded by colinear inputs on both sides. This requirement is enforced by inhibition, both within layer 4 (mediated by excitatory interlaminar input from layer 6), and within layer 2/3 (mediated by excitatory horizontal input at the disynaptic inhibitory interneurons). The model predicts that the bipole rule fails if either source of inhibition is lost. This prediction suggests that the selectivity of colinear facilitation is not just a property of layer 2/3, but rather a property of how intercellular interactions are balanced across several cortical layers.

Figure 13 (top) shows how a model layer 2/3 cell in case 3 is affected as the layer 6-to-4 inhibition is reduced. If this happens, then layer 4 cells can be activated solely by input from layer 6 because layer 6-to-4 excitation becomes stronger than 6-to-4 inhibition. If the W^+ inhibitory kernel (see equation 21) is reduced by 50%, then the bipole rule is still maintained. However, if it is reduced by 60%, then the layer 2/3 cell becomes

suprathreshold and the bipole property is lost. This means that layer 4 cells without bottom-up input can become activated by excitatory feedback via layers 2/3-to-5-to-6-to-4. Destroying the balance of excitation and inhibition between layers 6-to-4 enable this feedback to act like a spurious bottom-up input, thereby leading to a slow spread of activity away from all line ends and corners. This simulation dramatizes the importance of balancing the layer 6-to-4 on-center and off-surround so that its main effects on layer 4 are either to modulate the excitability of layer 4 cells in the on-center or to strongly inhibit the activation of layer 4 cells in the surround. The simulation hereby provides a strong test of the model's ability to self-organize connections that maintain this balance.

Figure 13 (bottom) shows a similar result if disynaptic inhibition within layer 2/3 is reduced. If the T^* inhibitory kernel (see equation 26) is reduced by 30%, the unsupported cell remains subthreshold. If T^* is reduced by 50%, then the cell becomes suprathreshold, but stabilizes at a low firing rate, and so the bipole property is partially retained. If T^* is reduced by 60%, then the cell becomes more active, and the bipole property is completely lost. This again leads to a slow spread of activity away from line ends and corners. These results show the importance of balancing excitation and inhibition within layer 2/3 to prevent the non-classical receptive fields from spreading activity non-selectively across the entire network. The results highlight that the model's ability to self-organize such selective connections is a real achievement, and that the model mechanisms are robust, since this balance can be maintained within a broad parameter range.

Destabilization of Development by Unbalanced Excitatory and Inhibitory Learning

Figure 13 shows that reducing the inhibitory kernels in layer 4 or layer 2/3 to about half their present values can lead to a loss of the bipole property. Once this happens, cortical development and adult perceptual learning can spiral out of control, as more excitatory learning (via equations 29 and 33) leads to greater average cortical activity, which in turn leads to more excitatory learning. Therefore, inhibitory learning that balances excitatory learning is needed to stabilize cortical development and learning, and, in so doing, cause the grouping properties with which we are familiar in the adult. The key parameters that guarantee network stability are C_3 in equation (38) and τ in equation (35).

These parameters need to be set so that the W^* and T^* kernels that regulate layer 4 and layer 2/3 inhibition, respectively, reach sufficiently large values. The results depicted in Figure 13 show why network development and learning is robust with regard to changes in these parameters, since the bipole property that maintains grouping, and thus learning, selectivity is maintained for a wide range of values in both inhibitory kernels.

Discussion

This article develops a neural model of how horizontal and interlaminar cortical connections in cortical areas V1 (and, by extension, area V2) develop in a stable fashion. Stable development is controlled by the growth of suitably balanced excitatory and inhibitory connections within layer 2/3 and between layers 6 and 4. The model grows connections that simulate key properties of developmental anatomical data and adult neurophysiological data. For example, as in other data (Calloway and Katz, 1990; Durack and Katz, 1996; Galuske and Singer, 1996), the model develops crude clustering of weak horizontal connections prior to patterned visual input. Visually patterned input strengthens horizontal connections while increasing their projection range and colinear orientational specificity. The growth of new and/or the retraction of pre-existing horizontal connections (Kandel and O'Dell, 1992; Antonini and Stryker, 1993b) is determined by activity-based competition for finite resources. The result is a network of horizontal connections in layer 2/3 between iso-orientation columns, which are biased along the preferred orientation (Fitzpatrick, 1996, Schmidt *et al.*, 1997) and whose classical receptive fields are much smaller than the extent of their horizontal connections (Das and Gilbert, 1995; Fitzpatrick, 1996).

Model development leads to a network that is capable of simulating adult psychophysical data about context-sensitive perceptual grouping, notably data that depend upon non-classical receptive field properties. Further simulations of adult psychophysical data can be found elsewhere (Grossberg *et al.*, 1997; Grossberg and Raizada, 2000; Raizada and Grossberg, 2000). One of the model's key lessons is that the same mechanisms which stabilize development also control properties of perceptual grouping and learning in the adult. In particular, connections which grew to stably reflect robust statistical properties of the visual world *define* the properties of adult perceptual grouping as we know them. We claim that these grouping properties help to dynamically maintain the match between world statistics and the brain's ability to process them.

As noted above, in both the brain and the model, layer 2/3 boundary signals feed back via connections to layer 6 via layer 5 (Gilbert and Wiesel, 1979; Ferster and Lindström, 1985). Layer 6, in turn, activates the on-center off-surround network from layer 6-to-4. This feedback has been called *folded feedback* (Grossberg, 1999) because the feedback signals from layer 2/3 to layer 6 get transmitted in a feedforward fashion back to layer 4 and thereupon to layer 2/3. The feedback is hereby 'folded' back into the feedforward flow of bottom-up information within the laminar cortical circuits. Folded feedback links cells in layers 2/3, 6, 5 and 4 into functional columns (Mountcastle, 1957; Hubel and Wiesel, 1962, 1977). In so doing, it enables the strongest grouping signals in layer 2/3 to use the on-center off-surround network from layer 6-to-4 to reinforce the strongest groupings and to inhibit weaker groupings, during both early development and adult grouping and learning.

The 6-to-4 folded feedback pathway is thus predicted to do several things: (i) maintain contrast sensitivity to bottom-up inputs from LGN; (ii) help to select the strongest groupings that initially get formed in layer 2/3; (iii) receive top-down attentional modulation from V2 and other cortical areas; and (iv) deliver top-down attentional signals to LGN. The spatial scale of the inhibition from layer 6-to-4, being smaller than the spatial extent of the excitatory horizontal connections within layer 2/3, and larger than the disynaptic inhibition within layer 2/3 that maintains the bipole grouping property, is well-suited to these tasks. In particular, the model uses this pathway to simulate how attention can propagate along a curve (Grossberg and Raizada, 2000), as found in neurophysiological recordings from macaque area V1 (Roelfsema *et al.*, 1998), thereby illustrating how attention can selectively enhance an entire object. This layer 6-to-4 on-center off-surround attentional circuit in the model also clarifies other important properties of attention, such as its on-center off-surround characteristics (Bullier *et al.*, 1996) and the property that the V1 layer whose activation is most reduced by cutting off V2 feedback is layer 6 (Sandell and Schiller, 1982). An interface in layer 6 for top-down attention also clarifies how attention can, in principle, propagate across multiple brain

regions via layer 6-to-6 top-down connections, modulating each target cortical area without fully activating, or driving, its grouping cells.

The model provides a mechanistic account of how adult perceptual learning and the plasticity of cortical representations after lesions may arise from developmental mechanisms when the dynamic equilibrium between input statistics and cortical circuitry is upset (Grossberg, 1980; Merzenich *et al.*, 1988; Carpenter and Grossberg, 1991; Karni and Sagi, 1991; Bailey *et al.*, 1992; Gilbert and Wiesel, 1992; Kandel and O'Dell, 1992; Mayford *et al.*, 1992; Poggio *et al.*, 1992; Zohary *et al.*, 1994). As noted above, the model predicts that the stability of model development and adult learning requires an approximate balance between excitation and inhibition within layer 2/3 and between layers 6 and 4.

In particular, the model predicts that the balanced layer 6-to-4 on-center off-surround circuit *modulates* layer 4 cells, but cannot, by itself, fully activate them. This prediction is consistent with neurophysiological data from ferret visual cortex showing that the layer 6-to-4 circuit is functionally weak (Wittmer *et al.*, 1997). The model also predicts that the layer 6-to-4 modulatory circuit is used by top-down signals from higher cortical areas to attentionally prime layer 4 cells in area V1, without fully activating them (Grossberg, 1999). Thus the same modulatory property that is needed to ensure stable development is predicted to control the ability of higher-order processes to attentionally prime lower areas, without fully activating them. The rules of stable development are thus predicted to define what we *mean* by adult attention, as well as adult grouping and learning. This hypothesis is consistent with neurophysiological data of Hupé *et al.* who have shown that 'feedback connections from area V2 modulate but do not create center-surround interactions in V1 neurons' (Hupé *et al.*, 1997). Such intercortical feedback connections from V2 to V1 can modulate the circuits of V1 with 'higher-order' boundary completion and figure-ground perception properties of area V2 (Grossberg, 1994, 1997; Lamme, 1995; Zipser *et al.*, 1996), and/or other cortical areas (Hupé *et al.*, 1998; Watanabe *et al.*, 1998). Taken together, these properties open the way towards a unified mechanistic model of infant cortical development and adult neurophysiology, perceptual grouping, attention and learning.

The model hereby provides a simple functional explanation of why there are direct bottom-up inputs to layer 4, as well as indirect bottom-up inputs to layer 4 via layer 6, in many cortical areas (van Essen and Maunsell, 1983; Felleman and van Essen, 1991). The proposed explanation is that direct inputs to layer 4 are needed to supraliminally activate layer 4 cells because the indirect layer 6-to-4 inputs cannot do so: they must be merely modulatory in order to stabilize cortical development and learning.

Comparison with Other Models

It is informative to compare the properties of our developed model and its precursors (Grossberg and Mingolla, 1985, 1987; Gove *et al.*, 1995; Grossberg *et al.*, 1997) with alternative models of visual cortex and perceptual grouping. The present model's grouping properties have several advantages over those proposed by other computational models of visual cortex. Models which do not address the formation of illusory contours (Stemmler *et al.*, 1995; Li, 1998; Somers *et al.*, 1998; Yen and Finkel, 1998) not only fail to account for neurophysiological data (von der Heydt *et al.*, 1984; Sheth *et al.*, 1996) but also are unable to exploit the computational advantages that follow from closing incomplete boundaries: use of closure to guide surface reconstruction, boundary completion over the blind-spot and retinal veins, and more complete information for the recognition of partially occluded objects (Grossberg, 1994). Layer 2/3 bipole cells in the present model (Figure 1*c*) respond to both real and illusory contour stimuli of similar orientations, consistent with neurophysiological data (Sheth *et al.*, 1996), and are connected by horizontal axons which are coaxial with the receptive fields' preferred orientation (Bosking *et al.*, 1997; Schmidt *et al.*, 1997a), not orthogonal, as has also been proposed (Peterhans and von der Heydt, 1991). Because groupings are explicitly represented by connected regions of above-threshold layer 2/3 firing, the model shows how a high-contrast item can group with its neighbors while still having its net neural response suppressed by their presence, as found by Polat and co-workers (Polat *et al.*, 1998) [see Grossberg and Raizada for simulations of such data (Grossberg and Raizada, 2000).] Models in which grouping is represented only by lateral facilitation (Somers *et al.*, 1998; Stemmler *et al.*, 1995) cannot account for this, and force the paradoxical conclusion that high-contrast items would never group with each other, which is demonstrably not the case (Elder and Zucker, 1998). The present model's representation of grouping as distinct from visible stimulus contrast [as reviewed by Grossberg (Grossberg, 1994)] also receives support from recent psychophysical work (Hess *et al.*, 1998).

The Li model, in particular, uses bipole-like grouping cells in a single-layer recurrent network (Li, 1998). The surround inhibition originating from layer 6 in our model produces important functionality which is lacking in Li's model. Due to surround inhibition in both layer 4 and LGN, instigated by input from layer 6, our model performs spatial contrast enhancement on the boundary representation. The surround inhibition enhances boundaries at line ends and corners, setting the stage for the formation of illusory contours perpendicular to discontinuities. Li (Li, 1998) also considers synchronous oscillations during grouping of a type that has earlier been simulated in precursors of the present model (Grossberg and Somers, 1991), leading to quantitative simulations of human psychophysical data that may be linked to such oscillations (Grossberg and Grunewald, 1997).

Many predictions follow from our model and its extension to V2 (Grossberg, 1999; Grossberg and Raizada, 2000). For example: test if top-down V1 to LGN feedback helps to stabilize the development of disparity tuning in V1 during the visual critical period; test if a long-range horizontal grouping in layer 2/3 of V2 can inhibit vertically oriented simple cells at the midpoint of this grouping in layer 4 of V1; and test if layer 4 simple cells cannot be supraliminally activated if only the LGN-to-6-to-4 input pathway is active.

In their No Strong Loops Hypothesis, Crick and Koch (Crick and Koch, 1998) suggested that 'a strong excitatory [feedback] loop would throw the cortex into uncontrolled oscillations, as in epilepsy' (p. 248). They used this argument to suggest why modulatory brain circuits exist. However, there are many mathematical theorems which prove that neural networks with strong excitatory feedback can readily converge to stable patterns of activation that do not oscillate (Grossberg, 1969, 1973, 1978b, 1978c, 1980a; Ellias and Grossberg, 1975; Grossberg and Levine, 1975; Cohen and Grossberg, 1983; Hopfield, 1984). We propose that the reasons for modulatory circuits are more subtle than the Crick–Koch hypothesis: such circuits help to stabilize development in the infant and learning in the adult (Ito *et al.*, 1998).

We propose that variants of these laminar circuits may be used

in other perceptual and cognitive systems to achieve self-stabilizing learning and development. For example, long-range horizontal connections are known to occur in the auditory and language areas of human temporal cortex (Schmidt *et al.*, 1997b). Specializations of these connections may be used to group information in several neocortical areas. The present results may thus be viewed as a first step towards showing how laminar neocortex develops and learns connections and weights with which to optimally carry out many information-processing tasks.

Notes

S.G. supported in part by the Defense Advanced Research Projects Agency and the Office of Naval Research (ONR N00014-95-1-0409), the National Science Foundation (NSF IRI-97-20333), and the Office of Naval Research (ONR N00014-95-1-0657). J.R.W. supported in part by the Defense Advanced Research Projects Agency and the Office of Naval Research (ONR N00014-95-1-0409).

Address correspondence to Professor Stephen Grossberg, Department of Cognitive and Neural Systems, Boston University, 677 Beacon Street, Boston, MA 02215, USA. Email: steve@cns.bu.edu.

References

Ahmed B, Anderson JC, Douglas RJ, Martin KAC, Charmaine Nelson J (1994) Polyneuronal innervation of spiny stellate neurons in cat visual cortex. J Comp Neurol 341:39–49.

Ahmed R, Anderson JC, Douglas RJ, Martin KAC, Charmaine Nelson J (1994) Polyneuronal innervation of spiny stellate neurons in cat visual cortex. J Comp Neurol 341:39–49.

Ahmed R, Anderson JC, Martin KAC, Charmaine Nelson J (1997) Map of the synapses onto layer 4 basket cells of the primary visual cortex of the cat. J Comp Neurol 380:230–242.

Alonso J-M, Martinez LM (1998) Functional connectivity between simple cells and complex cells in cat striate cortex. Nature Neurosci 1:395–403.

Antonini A, Stryker MP (1993a) Functional mapping of horizontal connections in developing ferret visual cortex: experiments and modeling. J Neurosci 14:7291–7305.

Antonini A, Stryker MP (1993b) Rapid remodeling of axonal arbors in the visual cortex. Science 260:1819–1821.

Bailey CH, Kandel ER (1993) Structural changes accompanying memory storage. Annu Rev Physiol 55:397–426.

Bailey CH, Chen M, Keller F, Kandel ER (1992) Serotonin-mediated endocytosis of a pCAM: an early step of learning-related synaptic growth in aplysia. Science 256:645–649.

Beck J, Prazdny K, Rosenfeld A (1983) A theory of textural segmentation. In: Human and machine vision (Beck J, Hope B, Rosenfeld A, eds), pp. 1–38. New York: Academic Press.

Bolz J, Castellani V, Mann F, Henke-Fahle S (1996) Specification of layer-specific connections in the developing cortex. Progr Brain Res 108:41–54.

Born RT, Tootell RB (1991) Single-unit and 2-deoxyglucose studies of side inhibition in macaque striate cortex. Proc Natl Acad Sci USA 88:7071–7075.

Bosking W, Zhang Y, Schofield B, Fitzpatrick D (1985) Intrinsic connections of macaque striate cortex: axonal projections of cells outside lamina 4C. J Neurosci 5:3350–3369.

Bullier J, Hupé JM, James A, Girard P (1996) Functional interactions between areas V1 and V2 in the monkey. J Physiol (Paris) 90:217–220.

Callaway EM (1998) Prenatal development of layer-specific local circuits in primary visual cortex of the macaque monkey. J Neurosci 18:1505–1527.

Callaway EM, Katz LC (1990) Emergence and refinement of clustered horizontal connections in cat striate cortex. J Neurosci 10:1134–1153.

Callaway EM, Katz LC (1991) Effects of binocular deprivation on the development of clustered horizontal connections in cat striate cortex. Proc Natl Acad Sci USA 88:745–749.

Cannon MW, Fullenkamp SC (1993) Spatial interactions in apparent contrast: individual differences in enhancement and suppression effects. Vis Res 33:1685–1695.

Carpenter G, Grossberg S (1991) Pattern recognition by self-organizing neural networks. Cambridge, MA: MIT Press.

Chapman B, Stryker MP (1993) Development of orientation selectivity in ferret visual cortex and effects of deprivation. J Neurosci 13:5251-5262.

Chapman B, Zahs KR, Stryker MP (1991) Relation of cortical cell orientation selectivity to alignment of receptive fields of the geniculocortical afferents that arborize within a single orientation column in ferret visual cortex. J Neurosci 11:1347–1358.

Chino YM, Kaas JH, Smith EL III, Langston AL, Cheng H (1992) Rapid reorganization of cortical maps in adult cats following restricted deafferentation in retina. Vis Res 32:789–796.

Cohen MA, Grossberg S (1983) Absolute stability of global pattern formation and parallel memory storage by competitive neural networks. IEEE Trans Syst Man Cybernet SMC-13:815–826.

Crick F, Koch C (1998) Constraints on cortical thalamic projections: the no-strong-loops hypothesis. Nature 391:245–250.

Dalva MB, Katz LC (1994) Rearrangements of synaptic connections in visual cortex revealed by laser photostimulation. Science 265: 255–258.

Darian-Smith C, Gilbert CD (1994) Axonal sprouting accompanies functional reorganization in adult cat striate cortex. Nature 368:737–740.

Das A, Gilbert CD (1995) Long-range horizontal connections and their role in cortical reorganization revealed by optical recording of cat primary visual cortex. Nature 375:780–784.

Douglas RJ, Martin KAC, Whitteridge D (1989) A canonical microcircuit for neocortex. Neural Comput 1:480–488.

Douglas RJ, Koch C, Mahowald M, Martin KAC, Suarez HH (1995) Recurrent excitation in neocortical circuits. Science 269:981–985.

Dresp B, Grossberg S (1997) Contour integration across polarities and spatial gaps: from local contrast filtering to global grouping. Vis Res 37:913–924.

Durack JC, Katz LC (1996) Development of horizontal projections in layer 2/3 of ferret visual cortex. Cereb Cortex 6:178–183.

Durbin R, Mitchison G (1990) A dimension reduction framework for understanding cortical maps. Nature 343:644–647.

Elder JH, Zucker S (1998) Evidence for boundary-specific grouping. Vis Res 38:143–152.

Ellias SA, Grossberg S (1975) Pattern formation, contrast control, and oscillations in the short term memory of shunting on-center off-surround networks. Biol Cybernet 20:69–98.

Felleman DJ, van Essen DC (1991) Distributed hierarchical processing in the primate cerebral cortex. Cereb Cortex 1:1–47.

Ferster D (1988) Spatially opponent excitation and inhibition in simple cells of the cat visual cortex. J Neurosci 8:1172–1180.

Ferster D, Lindström S (1985) Synaptic excitation of neurones in area 17 of the cat by intracortical axon collaterals of cortico-geniculate cells. J Physiol 367:233–252.

Field DJ, Hayes A, Hess RF (1993) Contour integration by the human visual system: evidence for a local 'association field'. Vis Res 33:173–193.

Fitzpatrick D (1996) The functional organization of local circuits in visual cortex: insights from the study of tree shrew striate cortex. Cereb Cortex 6:329- 341.

Galuske RAW, Singer W (1996) The origin and topography of long-range intrinsic projections in cat visual cortex: a developmental study. Cereb Cortex 6:417–430.

Gilbert CD (1992) Horizontal integration and cortical dynamics. Neuron 9:1–13.

Gilbert CD, Wiesel TN (1979) Morphology and intracortical projections of functionally characterised neurones in the cat visual cortex. Nature 280:120–125.

Gilbert CD, Wiesel TN (1989) Columnar specificity of intrinsic horizontal and corticocortical connections in cat visual cortex. J Neurosci 9:2432–2442.

Gilbert CD, Wiesel TN (1992) Receptive field dynamics in adult primary visual cortex. Nature 356:150–152.

Gove A, Grossberg S Mingolla E (1995) Brightness perception, illusory contours, and corticogeniculate feedback. Vis Neurosci 12:1027–1052.

Grieve KL Sillito AM (1991a) The length summation properties of layer VI cells in the visual cortex and hypercomplex cell end zone inhibition. Exp Brain Res 84:319–325.

Grieve KL Sillito AM (1991b) A re-appraisal of the role of layer VI of the visual cortex in the generation of cortical end inhibition. Exp Brain Res 87:521–529.

Grieve KL, Sillito AM (1995) Non-length-tuned cells in layers II/III and IV

of the visual cortex: the effect of blockade of layer VI on responses to stimuli of different lengths. Exp Brain Res 104:12–20.
Grinvald A, Lieke EE, Frostig RD, Hildesheim R (1994) Cortical point-spread function and long-range lateral interactions revealed by real-time optical imaging of macaque monkey primary visual cortex. J Neurosci 14:2545–2568.
Grosof DH, Shapley RM, Hawken MJ (1993) Macaque V1 neurons can signal 'illusory' contours. Nature 365:550–552.
Grossberg S (1968) Some nonlinear networks capable of learning a spatial pattern of arbitrary complexity. Proc Natl Acad Sci USA 59:368–372.
Grossberg S (1969) On learning and energy-entropy dependence in recurrent and nonrecurrent signed networks. J Statist Phys 1:319–350.
Grossberg S (1973) Contour enhancement, short-term memory, and constancies in reverberating neural networks. Stud Appl Math 52:217–257.
Grossberg S (1976a) Adaptive pattern classification and universal recoding. I: Parallel development and coding of neural feature detectors. Biol Cybernet 23:121–134.
Grossberg S (1976b) Adaptive pattern classification and universal recoding. II: Feedback, expectation, olfaction, and illusions. Biol Cybernet 23:187–202.
Grossberg S (1978a) Communication, memory, and development. In: Progress in theoretical biology (Rosen R, Snell F, eds), Vol. 5, pp. 233–374. New York: Academic Press.
Grossberg S (1978b) Competition, decision, and consensus. J Math Anal Applic 66:470–493.
Grossberg S (1978c) Decisions, patterns, and oscillations in nonlinear competitive systems with applications to Volterra–Lotka systems. J Theor Biol 73L101–130.
Grossberg S (1980a) Biological competition: decision rules, pattern formation, and oscillations. Proc Natl Acad Sci USA 77:2338–2342.
Grossberg S (1980b) How does a brain build a cognitive code? Psychol Rev 87:1–51.
Grossberg S (1982) Studies of mind and brain. Amsterdam: Kluwer.
Grossberg S (1983) The quantized geometry of visual space: the coherent computation of depth, form, and lightness. Behav Brain Sci 6:625–657.
Grossberg S (1984) Outline of a theory of brightness, color, and form perception. In: Trends in mathematical psychology (Degreef E, van Buggenhaut J, eds). Amsterdam: North-Holland.
Grossberg S (1994) 3-D vision and figure–ground separation by visual cortex. Percept Psychophys 55:48–120.
Grossberg S (1997) Cortical dynamics of 3-D figure-ground perception of 2-D pictures. Psychol Rev 104:618–658.
Grossberg S (1999) How does the cerebral cortex work? Learning, attention, and grouping by the laminar circuits of visual cortex. Spatial Vis 12:163–185.
Grossberg S, Levine D (1975) Some developmental and attentional biases in the contrast enhancement and short term memory of recurrent neural networks. J Theor Biol 53:341–380.
Grossberg S, Mingolla E (1985) Neural dynamics of perceptual grouping: textures, boundaries, and emergent segmentations. Percept Psychophys 38:141–171.
Grossberg S, Mingolla E (1987) Neural dynamics of surface perception: boundary webs, illuminants, and shape-from-shading. Comput Vis Graph Image Process 37:116–165.
Grossberg S, Somers DC (1991) Synchronized oscillations during cooperative feature linking in a cortical model of visual perception. Neural Networks 4:453–466.
Grossberg S, Olson S (1994) Rules for the cortical map of ocular dominance and orientation columns. Neural Networks 7:883–894.
Grossberg S, Grunewald A (1997) Cortical synchronization and perceptual framing. J Cogn Neurosci 9:117–132.
Grossberg S, McLaughlin N (1997) Cortical dynamics of 3-D surface perception: binocular and half-occluded scenic images. Neural Networks 10:1583–1605.
Grossberg S, Williamson JR (1997) Linking cortical development to visual perception. Soc Neurosci Abstr 23:568.
Grossberg S, Pessoa L (1998) Texture segregation, surface representation, and figure–ground separation. Vis Res 38:137–161.
Grossberg S, Raizada RDS (2000) Contrast-sensitive perceptual grouping and object-based attention in the laminar circuits of primary visual cortex. Vis Res 40:1413–1432.
Grossberg S, Mingolla E, Ross WD (1997) Visual brain and visual perception: how does the cortex do perceptual grouping? Trends Neurosci 20:106–111.
Grunewald A, Grossberg S (1998) Self-organization of binocular disparity tuning by reciprocal corticogeniculate interactions. J Cogn Neurosci 10:199–215.
Gundersen RW, Barrett JN (1979) Neuronal chemotaxis: chick dorsal-root axons turn toward high concentrations of nerve growth factor. Science 206:1079–1080.
Gundersen RW, Barrett JN (1980) Characterization of the turning response of dorsal root neurites toward nerve growth factor. J Cell Biol 87:546–554.
Heeger DJ (1993) Modeling simple-cell direction selectivity with normalized, half-squared, linear operators. J Neurophysiol 70:1885–1898.
Hess G, Donoghue JP (1994) Long-term potentiation of horizontal connections provides a mechanism to reorganize cortical maps. J Neurophysiol 71:2543–2547.
Hess RF, Dakin SC, Field DJ (1998) The role of 'contrast enhancement' in the detection and appearance of visual contours. Vis Res 38:783–787.
Hirsch JA, Gilbert CD (1991) Synaptic physiology of horizontal connections in the cat's visual cortex. J Neurosci 11:1800–1809.
Hodgkin AL (1964) The conduction of the nervous impulse. Thomas: Springfield, IL.
Hopfield JJ (1984) Neurons with graded response have collective computational properties like those of two-state neurons. Proc Natl Acad Sci 81:3088–3092.
Hubel DH, Wiesel TN (1962) Receptive fields, binocular interaction and functional architecture in the cat's visual cortex. J Physiol 160:106–154.
Hubel DH, Wiesel TN (1963) Shape and arrangement of columns in cat's striate cortex. J Physiol 195:215–243.
Hubel DH, Wiesel TN (1968) Receptive fields and functional architecture of monkey striate cortex. J Physiol 195:215–243.
Hubel DH, Wiesel TN (1977) Functional architecture of macaque monkey visual cortex. Proc R Soc Lond B 198:1–59.
Hupé JM, James AC, Girard DC, Bullier J (1997) Feedback connections from V2 modulate intrinsic connectivity within V1. Soc Neurosci Abstr 406.15 1031.
Hupé JM, James AC, Payne BR, Lomber SG, Bullier J (1998) Cortical feedback improves discrimination between figure and background by V1, V2 and V3 neurons. Nature 394:784–787.
Innocenti GM (1981) Growth and reshaping of axons in the establishment of visual callosal connections. Science 212:824–827.
Innocenti GM, Frost DO (1979) Effects of visual experience on the maturation of the efferent system to the corpus callosum. Nature 280:231–233.
Ito M, Westheimer G, Gilbert CD (1998) Attention and perceptual learning modulate contextual influences on visual perception. Neuron 20:1191–1197.
Julesz B (1971) Foundations of cyclopean perception. Chicago, IL: University of Chicago Press.
Kalarickal GJ, Marshall JA (1999) Models of receptive-field dynamics in visual cortex. Vis Neurosci 16:1055–1081.
Kandel ER O'Dell TJ (1992) Are adult learning mechanisms also used for development? Science 258 243–246.
Kanizsa G (1979) Organization in vision. New York: Praeger.
Kanizsa G (1985) Seeing and thinking. Acta Psychol 59:23–33.
Kapadia MK, Gilbert CD, Westheimer G (1994) A quantitative measure for short-term cortical plasticity in human vision. J Neurosci 14:451–457.
Kapadia MK, Ito M, Gilbert CD, Westheimer G (1995) Improvement in visual sensitivity by changes in local context: parallel studies in human observers and in V1 of alert monkeys. Neuron 15:843–856.
Karni A, Sagi D (1991) Where practice makes perfect in textural discrimination: evidence for primary visual cortex plasticity. Proc Natl Acad Sci USA 88, 4966–4970.
Katz LC, Callaway EM (1992) Development of local circuits in mammalian visual cortex. Annu Rev Neurosci 15:31–56.
Kisvarday ZF, Beaulieu C, Eysel UT (1993) Network of GABAergic large basket cells in cat visual cortex (area 18): implication for lateral disinhibition. J Comp Neurol 327:398–415.
Kisvarday ZF, Kim DS, Eysel UT, Bonhoeffer T (1994) Relationship between lateral inhibitory connections and the topography of the orientation map in cat visual cortex. Eur J Neurosci 6:1619–1632.
Kisvarday ZF, Toth E, Rausch M, Eysel UT (1995) Comparison of lateral excitatory and inhibitory connections in cortical orientation maps of the cat. Soc Neurosci Abstr 21:907.

Knierim JJ, van Essen DC (1992) Neuronal responses to static texture patterns in area V1 of the alert macaque monkey. J Neurophysiol 67:961–980.
Kohonen T (1989) Self-organization and associative memory, 3rd edn. Berlin: Springer-Verlag.
Lamme VAF (1995) The neurophysiology of figure–ground segregation in primary visual cortex. J Neurosci 15:1605–1615.
Lesher GW, Mingolla E (1993) The role of edges and line-ends in illusory contour formation. Vis Res 33:2253–2270.
Letourneau PC (1978) Chemotactic response of verve fiber elongation to nerve growth factor. Dev Biol 66:183–196.
Li Z (11998). A neural model of contour integration in the primary visual cortex. Neural Comput 10:903–940.
Lichtman JW, Purves D (1981) Regulation of the number of axons that inervate target cells. In: Development in the nervous system (Garrod DR, Feldman JD, eds), pp. 233–243. Cambridge: Cambridge University Press,.
Linsker R (1986a) From basic network principles to neural architecture. Emergence of spatial-opponent cells. Proc Natl Acad Sci USA 83:7508–7512.
Linsker R (1986b) From basic network principles to neural architecture. Emergence of spatial-opponent cells. Proc Natl Acad Sci USA 83:8390–8394.
Liu Z, Gaska JP, Jacobson LD, Pollen DA (1992) Interneuronal interaction between members of quadrature phase and anti-phase pairs in the cat's visual cortex. Vis Res 32:1193–1198.
Löwel S, Singer W (1992) Selection of intrinsic horizontal connections in the visual cortex by correlated neuronal activity. Science 255:209–212.
Löwel S Singer W (1992) Neuronal responses to static texture patterns in area V1 of the alert macaque monkey. J Neurophysiol 67:961–980.
Luhmann HJ, Millan LM, Singer W (1986) Development of horizontal intrinsic connections in cat striate cortex. Exp Brain Res 63:443–448.
Lund JS Yoshioka T (1991) Local circuit neurons of macaque monkey striate cortex: III. Neurons of laminae 4B, 4A, and 3B. J Comp Neurol 311:234–258.
Mayford M, Barzilai A, Keller F, Schacher S, Kandel ER (1992) Modulation of an NCAM-related adhesion molecule with long-term synaptic plasticity in aplysia. Science 256:638–644.
McClurkin JW, Optican LM, Richmond BJ (1994) Cortical feedback increases visual information transmitted by monkey parvocellular lateral geniculate nucleus neurons. Vis Neurosci 11:601–617.
McGuire BA, Gilbert CD, Rivlin PK, Wiesel TN (1991) Targets of horizontal connections in macaque primary visual cortex. J Comp Neurol 305:370–392.
Merzenich MM, Recanzone EG, Jenkins WM, Allard TT, Nudo RJ (1988) In: Neurobiology of neocortex (Rakic P, Singer W, eds), pp. 41–67. New York: Wiley.
Miller KD (1992) Development of orientation columns via competition between on- and off-center inputs. NeuroReport 3:73–76.
Miller KD (1994) A model for the development of simple cell receptive fields and the ordered arrangement of orientation columns through activity-dependent competition between ON- and OFF-center inputs. J Neurosci 14:409–441.
Mountcastle VB (1957) Modality and topographic properties of single neurons of cats somatic sensory cortex. J Neurophysiol 20:408–434.
Murphy PC, Sillito AM (1987) Corticofugal feedback influences the generation of length tuning in the visual pathway. Nature 329:727–729.
Murphy PC and Sillito AM (1996) Functional morphology of the feedback pathway from area 17 of the cat visual cortex to the lateral geniculate nucleus. J Neurosci 16:1180–1192.
Obermayer K, Blasdel GG (1993) Geometry of orientation and ocular dominance columns in monkey striate cortex. J Neurosci 13:4114–4129.
Obermayer K, Ritter H, Schulten K (1990) A principle for the formation of the spatial structure of retinotopic maps, orientation and ocular dominance columns. Proc Natl Acad Sci USA USA 87:8345–8349.
Obermayer K, Blasdel GG, Schulten K (1992) Statistical–mechanical analysis of self-organization and pattern formation during the development of visual maps. Phys Rev A 45:7568–7589.
Olson SJ, Grossberg S (1998) A neural network model for the development of simple and complex cell receptive fields within cortical maps of orientation and ocular dominance. Neural Networks 11:189–208.
Palmer LA, Davis TL (1981) Receptive field structure in cat striate cortex. J Neurophysiol 46:260–276.
Peterhans E von der Heydt R (1989) Mechanisms of of contour perception in monkey visual cortex. II. Contours bridging gaps. J Neurosci 9:1749–1763.
Poggio T, Fahle M, Edelman S (1992) Fast perceptual learning in visual hyperacuity. Science 256:1018–1021.
Polat U, Sagi D (1993) Lateral interactions between spatial channels: suppression and facilitation revealed by lateral masking experiments. Vis Res 33:993–999.
Polat U, Sagi D (1994) The architecture of perceptual spatial interactions. Vis Res 34:73–78.
Polat U, Mizobe K, Pettet MW, Kasamatsu T, Norcia AM (1998) Collinear stimuli regulate visual responses depending on cell's contrast threshold. Nature 391:580–584.
Pollen DA, Ronner SF (1981) Phase relationships between adjacent simple cells in the visual cortex. Science 212:1409–1411.
Przybyszewski AW, Foote W, Pollen DA (1998) Contrast gain control of LGN neurons by V1. Invest Ophthalmol Vis Sci 39:S238.
Purves D, Lichtman JW (1980) Elimination of synapses in the developing nervous system. Science 210:153–157.
Raizada RDS, Grossberg S (2000) Context-sensitive binding by the laminar circuits of V1 and V2: a unified model of perceptual grouping, attention, and orientation contrast. Vis Cogn (in press).
Ramachandran VS (1976) Global grouping overrides point-to-point disparities. Perception 5:125–128.
Ramachandran VS Nelson JI (1976) Global grouping overrides point-to-point disparities. Perception 5:125–128.
Redies C, Crook JM, Creutzfeldt OD (1986) Neural responses to borders with and without luminance gradients in cat visual cortex and dLGN. Exp Brain Res 61:469–481.
Reid RC, Alonso, J-M. (1995) Specificity of monosynaptic connections from thalamus to visual cortex. Nature 378:281–284.
Ringach DL, Hawken MJ, Shapley R (1999) Properties of macaque V1 neurons studied with natural image sequences. Invest Ophthalmol Vis Sci 40:abstract 989.
Roelfsema PR, Lamme VAF, Spekreijse H (1998) Object-based attention in the primary visual cortex of the macaque monkey. Nature 395:376–381.
Rojer AS Schwartz EL (1989) A parametric model of synthesis of cortical column patterns. International Joint Conference on Neural Networks, Vol. 2, p. 603.
Rojer AS, Schwartz E (1990) Cat and monkey cortical columnar patterns modeled by band-pass-filtered 2d white noise. Biol Cybernet 62:381–391.
Ruthazer ES, Stryker MP (1996) The role of activity in the development of long-range horizontal connections in area 17 of the ferret. J Neurosci 15:7253–7269.
Sandell JH, Schiller PH (1982) Effect of cooling area 18 on striate cortex cells in the squirrel monkey. J Neurophysiol 48:38–48.
Schmid LM, Rosa MGP., Calford MB, Ambler JS (1996) Visuotopic reorganization in the primary visual cortex of adult cats following monocular and binocular retinal lesions. Cereb Cortex 6:388–405.
Schmidt KE, Goebel R, Löwel S, Singer W (1997a) The perceptual grouping criterion of colinearity is reflected by anisotropies of connections in the primary visual cortex. Eur J Neurosci 9:1083–1089.
Schmidt KE, Schlote W, Bratzke H, Rauen T, Singer W, Galuske RAW (1997b) Patterns of long range intrinsic connectivity in auditory and language areas of the human temporal cortex. Soc Neurosc Abstr 415.13, 1058.
Shadlen MN, Newsome WT (1998) The variable discharge of cortical neurons: implications for connectivity, computation, and information coding. J Neurosci 18:3870–3896.
Sheth BR, Sharma J, Rao SC, Sur M (1996) Orientation maps of subjective contours in visual cortex. Science 274:2110–2115.
Shipley TF, Kellman PJ (1992) Strength of visual interpolation depends on the ratio of physically specified to total edge length. Percept Psychophys 52:97–106.
Sillito AM, Jones HE, Gerstein GL, West DC (1994) Feature-linked synchronization of thalamic relay cell firing induced by feedback from the visual cortex. Nature 369:479–482.
Sillito AM, Grieve KL, Jones HE, Cudeiro J, Davis J (1995) Visual cortical mechanisms detecting focal orientation discontinuities. Nature 378:492–496.

Sirosh J Miikkulainen R (1994) Cooperative self-organization of afferent and lateral connections in cortical maps. Biol Cybernet 71:66–78.
Sobiano M, Spillman L, Bach M (1996) Vis Res 36:109–116.
Somers DC, Nelson SB, Sur M (1995) An emergent model of orientation selectivity in cat visual cortical simple cells. J Neurosci 15:5448–5465.
Somers DC, Todorov EV, Siapas AG, Toth LJ, Kim D, Sur M (1998) A local circuit approach to understanding integration of long-range inputs in primary visual cortex. Cereb Cortex 8:204–217.
Stratford KJ, Tarczy-Hornoch K, Martin KAC., Bannister NJ, Jack JJB (1996) Excitatory synaptic inputs to spiny stellate cells in cat visual cortex. Nature 382:258–261.
Stemmler M, Usher M, Niebur E (1995) Lateral interactions in primary visual cortex: a model bridging physiology and psychophysics. Science 269:1877–1880.
Stryker MP, Harris WA (1986) Binocular impulse blockade prevents the formation of ocular dominance columns in cat visual cortex. J Neurosci 6:2117–2133.
Swindale N (1980) A model for the formation of ocular dominance column stripes. Proc R Soc Lond B 208:243–264.
Swindale N (1982) A model for the formation of orientation columns. Proc R Soc Lond B 215:211–230.
Swindale N (1992) A model for the coordinated development of columnar systems in primate striate cortex. Biol Cybernet 66:217–230.
Usher M, Donnelly N (1998) Visual synchrony affects binding and segmentation in perception. Nature 394:179–182.
van Essen DC, Maunsell JHR (1983) Hierarchical organization and functional streams in the visual cortex. Trends Neurosci 6:370–375.
van Essen DC, Newsome WT, Maunsell JHR (1984) The visual representation in striate cortex of macaque monkey: asymmetries, anisotropies and individual variability. Vis Res 24:429–448.
van Vreeswijk C, Sompolinsky H (1998) Chaotic balanced state in a model of cortical circuits. Neural Comput 10:1321–1371.
von der Heydt R, Peterhans E (1989) Mechanisms of contour perception in monkey visual cortex. I. Lines of pattern discontinuity. J Neurosci 9:1731–1748.
von der Heydt R, Peterhans E, Baumgartner G (1984) Illusory contours and cortical neuron responses. Science 224:1260–1262.
von der Malsburg C (1973) Self-organization of orientation sensitive cells in the striate cortex. Kybernetik 14:85–100.
Watanabe T, Cavanagh P (1992) Depth capture and transparency of regions bounded by illusory and chromatic contours. Vis Res 32:527–532.
Watanabe T, Sasaki Y, Miyauchi S, Putz B, Fujimake N, Nielsen M, Takino R, Miyakawa S (1998) Attention-regulated activity in human primary visual cortex. J Neurophysiol 79:2218–2221.
Weber J, Kalil RE, Behan M (1989) Synaptic connections between corticogeniculate axons and interneurons in the dorsal lateral geniculate nucleus of the cat. J Comp Neurol 289:156–164.
Weliky M, Katz LC (1994) Functional mapping of horizontal connections in developing ferret visual cortex: experiments and modeling. J Neurosci 14:7291–7305.
Williamson JR, Grossberg S (1998) How cortical development leads to perceptual grouping in the laminar circuits of visual cortex. Invest Ophthalmol Vis Sci 39:S328.
Willshaw D, von der Malsburg C (1976) How patterned neural connections can be set up by self-organization. Proc R Soc Lond B 194:431–445.
Wittmer LL, Dalva MB, Katz LC (1997) Reciprocal interactions between layer 4 and layer 6 cells in ferret visual cortex. Soc Neurosci Abstr 651.5, 1668.
Woo TU, Niederer JK, Finlay BL (1996) Cortical target depletion and the developing lateral geniculate nucleus: implications for trophic dependence. Cereb Cortex 6:446–456.
Yen SC and Finkel LH (1998) Extraction of perceptually salient contours by striate cortical networks. Vis Res 38:719–741.
Zipser K, Lamme VAF, Schiller PH (1996) Contextual modulation in primary visual cortex. J Neurosci 16:7376–7389.
Zohary E, Cerebrini S, Britten KH, Newsome WT (1994) Neuronal plasticity that underlies improvement in perceptual performance. Science 263:1289–1292.

Appendix: Model Equations

Because the model represents several different types of known cell types and their connections, equations and parameters need to be defined for each of these processes. Wherever possible, the model differential equations were solved at equilibrium in response to a constant input in order to speed up processing. These approximations do not affect the reliability of the results.

Retina

At each retinal position (i,j), an ON cell activity u_{ij}^{+} is defined by an on-center off-surround network that possesses narrow on-center and Gaussian off-surround kernels (see Fig. 14a). An OFF cell activity u_{ij}^{-} is also defined by an off-center on-surround network with narrow off-center and Gaussian on-surround kernels. The retinal cell activities caused by the constant visual inputs I have the equilibrium values:

$$u_{ij}^{+} = I_{ij} - \sum_{pq} G_{pq}(i,j,\sigma_1) I_{pq} \tag{3}$$

and

$$u_{ij}^{-} = -I_{ij} + \sum_{pq} G_{pq}(i,j,\sigma_1) I_{pq} \tag{4}$$

where $G_{pq}(i,j,\sigma)$ denotes a two-dimensional Gaussian kernel:

$$G_{pq}(i,j,\sigma) = \frac{1}{2\pi\sigma^2} \exp\left\{-\frac{1}{2\sigma^2}\left[(p-i)^2 + (q-j)^2\right]\right\} \tag{5}$$

Lateral Geniculate Nucleus

The LGN ON cell activity v_{ij}^{+} and OFF cell activity v_{ij}^{-}, at each position (i,j) obey membrane equations (Hodgkin, 1964) that interact via on-center off-surround networks. As noted above, such a network realizes a contrast gain-control process which retains cell sensitivity to image contrasts while compensating for variable illumination and normalizing network activity (Grossberg, 1982, 1983):

$$\frac{1}{\delta_C}\frac{\mathrm{d}}{\mathrm{d}t} v_{ij}^{+} = -v_{ij}^{+} + \left(1 - v_{ij}^{+}\right)\left[u_{ij}^{+}\right]^{+}\left(1 + A_{ij}\right) - \left(v_{ij}^{+} + 1\right)B_{ij} \tag{6}$$

and

$$\frac{1}{\delta_C}\frac{\mathrm{d}}{\mathrm{d}t} v_{ij}^{-} = -v_{ij}^{-} + \left(1 - v_{ij}^{-}\right)\left[u_{ij}^{-}\right]^{+}\left(1 + A_{ij}\right) - \left(v_{ij}^{-} + 1\right)B_{ij} \tag{7}$$

In (4) and (5), the half-wave rectified retinal output signals ($[u_{ij}]^{+} = \max(u_{ij}, 0)$) are multiplicatively gain-controlled (Sillito *et al.*, 1994; Gove *et al.*, 1995; Przybyszewski *et al.*, 1998) by a top-down on-center off-surround network (see Fig. 1*d*). The excitatory on-center feedback

$$A_{ij} = C_1 \sum_{r} x_{ijr} \tag{8}$$

comes from all cell activities x_{ijr} within layer 6 of area V1 at the corresponding position (i,j) that are tuned to any orientation r. The inhibitory off-surround signals

$$B_{ij} = C_2 \sum_{pqr} G_{pq}(i,j,\sigma_1) x_{pqr} \tag{9}$$

come from activities x_{pqr} at nearby positions (p,q) and all orientations r via the Gaussian kernel shown in Figure 14*a*. This center-surround feedback from layer 6 selects those LGN cells which have succeeded in activating cortical cells. The feedback also strengthens LGN responses at line ends. This in turn strengthens cortical responses at line ends via feedforward signals from LGN to layers 4 and 6 of V1; see equations (20) and (22) below. When these line end responses are aligned in space, they can generate illusory contour groupings perpendicular to the line ends (see Fig. 9). For further discussion and simulations about how these LGN hypotheses explain anatomical, neurophysiological and psychophysical data, see Gove *et al.* (Gove *et al.*, 1995).

Cortical Simple Cells

Simple cell responses derive from arrays of ON cell and OFF cell outputs from the LGN (see Fig. 1*a*). These ON cell and OFF cell outputs are filtered by a pair of Gaussian receptive fields, with each Gaussian offset to the right (R) or left (L) of the simple cell oriented axis. For simplicity, only

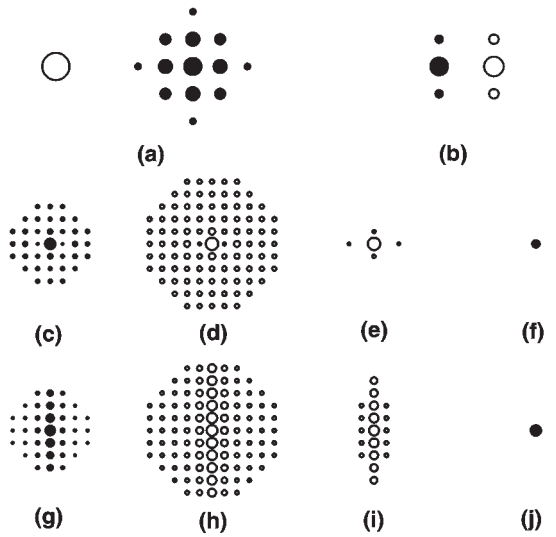

Figure 14. Spatial kernels used by model. Circle area denotes the size of a weight. Open circles denote excitatory weights and black circles denote inhibitory weights. Kernels (*a*) and (*b*) are prespecified; the remaining kernels start with zero values, and are learned. The kernels that govern interactions between vertically oriented cortical cells are shown. Kernels governing interactions with horizontally oriented cells are not shown. (*c*)–(*f*) depict the kernels following training in the unstructured vision phase (Fig. 2, left), and (*g*)–(*j*) depict the same kernels following training in the structured vision phase (Fig. 2, right). (*a*) Gaussian off-surround in equations (3), (6) and (7). (*b*) Vertical simple cell filter implemented in equation (14). (*c*,*g*) Layer 4 surround inhibitory weights, W^+, in equations (20) and (38). (*d*,*h*) Layer 2/3 axonal connection strengths, U, in equations (27), (29) and (30). (*e*,*i*) Layer 2/3 synaptic weights, V, in equations (27) and (33). (*f*,*j*) Layer 2/3 disynaptic inhibitory weights, T^+, in equations (26) and (36).

vertical and horizontal orientations were simulated. The Gaussians were defined by equation (5). The individual Gaussian inputs from LGN to layer 4 equal:

$$R^{\pm}_{ijk} = \sum_{pq}\left[v^{\pm}_{pq}\right]^+ G_{pq}(i+\sigma_2\sin\theta, j-\sigma_2\cos\theta,\sigma_2) \tag{10}$$

$$L^{\pm}_{ijk} = \sum_{pq}\left[v^{\pm}_{pq}\right]^+ G_{pq}(i-\sigma_2\sin\theta, j+\sigma_2\cos\theta,\sigma_2) \tag{11}$$

where $\theta = \pi k/2$, for the vertical orientations ($k = 1$) and the horizontal orientation ($k = 2$). Pairs of like-oriented, but spatially displaced, ON cell (R^+ or L^+) and OFF cell (L^- or R^-) inputs summate at each simple cell to form total LGN inputs of the form

$$S^R_{ijk} = R^+_{ijk} + L^-_{ijk} \tag{12}$$

$$S^L_{ijk} = R^-_{ijk} + L^+_{ijk} \tag{13}$$

Then these inputs mutually compete, as in the terms

$$\gamma\left[S^R_{ijk} - S^L_{ijk}\right]^+ \tag{14}$$

and

$$\gamma\left[S^L_{ijk} - S^R_{ijk}\right]^+ \tag{15}$$

Each pair of terms in (14) and (15) represents the responses of simple cells that have the same position (i,j) and orientation k, but are sensitive to opposite contrast polarities (see Fig. 14*b*).

In order to make the simulations manageable, some simplifications of known biological interactions were made. Even so, each simulation of model development (described below) took 11 days to run on a Silicon Graphics workstation. The simplifications that were made should not influence our results on cortical development or adult grouping. In particular, *in vivo* layer 4 simple cells that are sensitive to opposite contrast polarities pool their outputs at layer 2/3 complex cells (Alonso and Martinez, 1998). In order to cut the number of simulated cells in half, and with it the run time, we assumed that these simple cell outputs were pooled in layer 4:

$$C_{ijk} = \gamma\left[S^R_{ijk} - S^L_{ijk}\right]^+ + \gamma\left[S^L_{ijk} - S^R_{ijk}\right]^+ \tag{16}$$

In addition, we kept cell density as sparse as possible in order to reduce run time. This created well-known sparse sampling artifacts, such as a spatially coarser response of the simple and complex cells. These were corrected by subtracting a fraction of the overall difference between the net ON and OFF responses from the terms C_{ijk}. These extra terms can be eliminated in future simulations when faster computers are available. The total pooled term is thus:

$$\begin{aligned} C_{ijk} \;=\; & \gamma\left[S^R_{ijk} - S^L_{ijk}\right]^+ + \gamma\left[S^L_{ijk} - S^R_{ijk}\right]^+ \\ & -\omega\left[S^+_{ijk} - S^-_{ijk}\right]^+ - \omega\left[S^-_{ijk} - S^+_{ijk}\right]^+ \end{aligned} \tag{17}$$

where

$$S^+_{ijk} = R^+_{ijk} + L^+_{ijk} \tag{18}$$

and

$$S^-_{ijk} = R^-_{ijk} + L^-_{ijk} \tag{19}$$

The model assumes that layer 4 cell activities, y_{ijk}, are excited by the pooled LGN signal C_{ijk}. They also receive excitatory on-center input x_{ijk} from layer 6, and Gaussianly filtered off-surround input $\Sigma_{pqr} W^+_{pqrijk} m_{pqr}$ from layer 6 via layer 4 inhibitory interneurons (see Fig. 1*b*). In all:

$$\begin{aligned} \frac{1}{\delta_C}\frac{\mathrm{d}}{\mathrm{d}t} y_{ijk} \;=\; & -y_{ijk} + \left(1 - y_{ijk}\right)\left[C_{ijk} + \eta x_{ijk}\right] \\ & -\left(y_{ijk} + 1\right)\sum_{pqr} W^+_{pqrijk} m_{pqr} \end{aligned} \tag{20}$$

In the simulations, the equilibrium form of equation (20) was used:

$$y_{ijk} = \frac{C_{ijk} + \eta x_{ijk} - \sum_{pqr} W^+_{pqrijk} m_{pqr}}{1 + C_{ijk} + \eta x_{ijk} + \sum_{pqr} W^+_{pqrijk} m_{pqr}} \tag{21}$$

Layer 6 Cells

A layer 6 cell at position (i,j) and orientation k is assumed to receive oriented input, C_{ijk}, from LGN and feedback, z_{ijk}, from layer 2/3 complex pyramidal cells (see Fig. 1*b*). It is assumed that the C_{ijk} inputs are registered at layer 6 cells due to a prior stage of development during which LGN inputs learned an oriented connection to layer 6 cells due to correlations induced by layer 2/3-to-6 and/or layer 4-to-6 feedback from cells of both contrast polarities. Ringach *et al.* have reported that the responses of layer 6 cells in V1 do, in fact, exhibit a polarity-independent response component as well as a polarity-dependent component (Ringach *et al.*, 1999). In all, layer 6 cell activation, x_{ijk}, obeys:

$$\frac{1}{\delta_C}\frac{\mathrm{d}}{\mathrm{d}t} x_{ijk} = -x_{ijk} + \left(1 - x_{ijk}\right)\left[\alpha C_{ijk} + \phi F\left(z_{ijk}, \Gamma\right)\right] \tag{22}$$

The feedback signal function $F(\,)$ models the thresholded output signal of the layer 2/3 pyramidal cell activities z_{ijk}:

$$F\left(z_{ijk}, \Gamma\right) = \begin{cases} z_{ijk} & \text{if } z_{ijk} > \Gamma \\ 0 & \text{otherwise} \end{cases} \tag{23}$$

Function $F(\,)$ represents a simplified sigmoid signal function with a threshold at Γ. In the simulations, the equilibrium form of equation (22) was used:

$$x_{ijk} = \frac{\alpha C_{ijk} + \phi F\left(z_{ijk}, \Gamma\right)}{1 + \alpha C_{ijk} + \phi F\left(z_{ijk}, \Gamma\right)} \tag{24}$$

to speed up network convergence.

Layer 4 Inhibitory Interneurons

Layer 4 inhibitory interneuron activities, m_{ijk}, receive on-center input from layer 6 activities x_{ijk} and off-surround inhibition m_{pqr} from other layer 4 inhibitory interneurons:

$$\frac{1}{\delta_C}\frac{\mathrm{d}}{\mathrm{d}t}m_{ijk} = -m_{ijk} + \eta^2 x_{ijk}^2 - m_{ijk}\sum_{pqr} W^-_{pqrijk} m_{pqr} \tag{25}$$

The recurrent inhibition between layer 4 inhibitory interneurons helps to normalize their total output to the layer 4 simple cells. The on-center excitation x_{ijk}^2 is a quadratic term which allows excitation at layer 4 to dominate when layer 6 activity is low, and inhibition to dominate when layer 6 activity is high. This term plays a role like the high thresholds and steep activity functions of inhibitory neurons in the models of Stemmler *et al.* and Somers *et al.* (Stemmler *et al.*, 1995; Somers *et al.*, 1998).

Layer 2/3 Complex Cells and Long-range Horizontal Connections

In the adult model, layer 2/3 pyramidal cells receive excitatory input $[y_{ijk}]^+$ from layer 4 at the same position, excitatory input $\Sigma_{pqr}\ H_{pqrijk}\ F(z_{pqr},\Gamma)$ via the long-range horizontal kernels H_{pqrijk} from other layer 2/3 pyramidal cell signals $F(z_{pqr},\Gamma)$ at different positions, and inhibitory input $\Sigma_r T^+_{rk} s_{ijr}$ from the layer 2/3 disynaptic interneuronal activities s_{ijr} at the same position (i,j) and all orientations r (see Fig. 1*c*). Layer 2/3 pyramidal cells thus obey the equation:

$$\frac{1}{\delta_C}\frac{\mathrm{d}}{\mathrm{d}t}z_{ijk} = -z_{ijk} + \left(1 - z_{ijk}\right)\left(\lambda\left[y_{ijk}\right]^+ + \left[\sum_{pqr} H_{pqrijk} F\left(z_{pqr},\Gamma\right) - \sum_r T^+_{rk} s_{ijr}\right]^+\right) \tag{26}$$

The long-range horizontal excitatory connections H_{pqrijk} and short-range inhibitory connections T^+_{rk} in (26) both develop from zero initial values in the model. This developmental process has the property that unsupported cells which receive excitatory horizontal signals from only one direction are not activated enough to exceed threshold Γ, and thus are not able to propagate the grouping signal any further. Cells that receive sufficiently strong horizontal excitation from two sides, however, may exceed threshold and thereby contribute their own output to the grouping signal. These cells help to keep themselves and their neighbors above threshold in spite of the time-lagged rise in disynaptic inhibition. Nonlinear properties in layer 2/3 similar to those accomplished by signal $F(\ )$ in (23) have been reported elsewhere (Hirsch and Gilbert, 1991, Figure 3).

The horizontal connection strength, H_{pqrijk}, is the product of the axonal strength, U_{pqrijk}, from cell (p,q,r) to cell (i,j,k) and the synaptic weight, V_{pqrijk}, that abuts cell (i,j,k) after the axon from (p,q,r) contacts it. Thus:

$$H_{pqrijk} = U_{pqrijk}\ V_{pqrijk} \tag{27}$$

Layer 2/3 Disynaptic Inhibitory Interneurons

In the adult network, layer 2/3 inhibitory interneurons are excited by horizontal connections $\Sigma_{pqr}\ H_{pqrijk}\ F(z_{pqr},\Gamma)$ from layer 2/3 pyramidal cells, and are inhibited by layer 2/3 disynaptic interneuronal activities s_{ijr} that represent all orientations r at the same position (i,j). This recurrent inhibitory network tends to normalize the total output signal from each inhibitory interneuronal population:

$$\frac{1}{\delta_C}\frac{\mathrm{d}}{\mathrm{d}t}s_{ijk} = -s_{ijk} + \sum_{pqr} H_{pqrijk} F\left(z_{pqr},\Gamma\right) - s_{ijk}\sum_r T^-_{rk} s_{ijr} \tag{28}$$

Both the long-range horizontal connections H and the short-range inhibitory connections T^- in (28) develop from zero initial values in the model.

Parameters for Equations (3)–(28)

Cell activation parameters in all simulations, except those that were varied to demonstrate model robustness, are: $\sigma_1 = 1.0$, $\gamma = 10.0$, $\omega = 6.0$, $\Gamma = 0.1$, $C_1 = 1.5$, $C_2 = 0.075$, $\sigma_2 = 0.5$, $\delta_C = 0.25$, $\alpha = 0.5$, $\phi = 2.0$, $\eta = 2.0$, $\lambda = 1.25$.

Development of Layer 2/3 Excitatory Horizontal Axons

At the beginning of model development, layer 2/3 pyramidal cells have no horizontal axons. An intracellular process calibrates an amount of potential axonal growth, U_{total}. The variables U_{pqrijk} represent the strength of axonal connections from a layer 2/3 source cell at position (p,q) with orientational tuning r to a target cell at position (i,j) with orientational tuning k. At each position, there are four two-dimensional U kernels corresponding to the four orientational combinations of r and k (vertical-to-vertical, vertical-to-horizontal, etc.). These variables are initialized at zero, and updated via the equation

$$\frac{1}{\delta_A}\frac{\mathrm{d}}{\mathrm{d}t}U_{pqrijk} = F\left(z_{pqr},\Gamma\right)\left[\left(U_{\text{total}} - \sum_{IJK} U_{pqrIJK}\right) z_{ijk} A\left(E_{pqrijk}\right) - \psi U_{pqrijk}\sum_{IJK \neq ijk} z_{IJK} A\left(E_{pqrIJK}\right)\right] \tag{29}$$

in which z_{pqr} is the activity of the source cell; $F(z_{pqr},\Gamma)$ is the output signal from this cell, as defined in equation (23); z_{ijk} is the activity of the target cell; and z_{IJK} is the activity of other, competing, target cells. In equation (29), all axons from a given source cell compete for axonal resources, U_{total}, via the term $\Sigma_{IJK}\ U_{pqrIJK}$. This competition influences a source cell only when it is active enough to make its growth signal $F(z_{pqr},\Gamma)$ positive. There is thus an asymmetry, in that the source cell activity is thresholded, but the target cell activities are not. Similar asymmetries occur in equation (33) for learning excitatory synaptic weights and equation (35) for learning inhibitory synaptic weights. The reason for this asymmetry is that a cell's activity must be above threshold in order to influence other cells. In particular, a source cell's activity should be above threshold in order to alter its axonal connections or synaptic weights to target cells. Its pattern of axonal connections and synaptic weights should reflect the distribution of target cell activities when the source cell is capable of influencing them. On the other hand, a cell does not need to be above threshold in order to be influenced by other cells, and therefore there is no threshold requirement on target cells, governing the growth of connections to those cells.

When the source cell is above threshold, its axonal growth to a target cell is driven by activity-dependent morphogenetic gradients $z_{ijk}A(E_{pqrijk})$ in (29). Quantity E_{pqrijk} represents the distance between the axonal growth cone of source cell (p,q) and target cell (i,j). It is defined by the difference between the length κU_{pqrijk} of the growth cone and the distance D_{pqij} between the source cell and the target cell:

$$E_{pqrijk} = [D_{pqij} - \kappa U_{pqrijk}]^+ \tag{30}$$

The morphogenetic gradient $A(E_{pqrijk})$ that influences growth to cell (i,j,k) increases as the growth cone κU_{pqrijk} approaches (i,j,k), i.e. as E_{pqrijk} decreases. This property is captured by the equation:

$$A\left(E_{pqrijk}\right) = \frac{\beta}{\beta + E_{pqrijk}} \tag{31}$$

As $A(E_{pqrijk})$ increases, so too does the rate of axonal growth to cell (i,j,k), but only if its activity z_{ijk} is positive, as in (29).

Development of the connections U_{pqrijk} is restricted to a local, circular window, such that:

$$D_{pqij} < H_{\text{range}}/2 \tag{32}$$

Parameter H_{range} determines the spatial extent in which the growth of horizontal connections is possible. The actual extent of growth may be less than H_{range}. In our simulations, the horizontal connections grew to a length of nine iso-orientation columns (see Fig. 5). Figure 14*d*,*h* shows how the vertical-to-vertical U kernel has developed just before eye opening and after visual development self-equilibrates, respectively.

Equations (29)–(31) determine how, over time, activity correlations among layer 2/3 cells produce a spatial distribution of axonal connections. The four key parameters that influence this process are as follows. (i) Parameter U_{total} in (29) determines the total amount of axonal growth out of each layer 2/3 cell. (ii) Parameter ψ in (29) determines the

level of intracellular competition for axonal resources between different axons. Reducing ψ causes the distributions of axonal connections to become more isotropic. (iii) Parameter κ in equation (30) maps units of axon growth into units of spatial distance, in order to calculate the distance of an axon from its target. Increasing κ increases the length to which axons are capable of growing. (iv) Parameter β in (31) affects the shape of the chemical gradient that attracts an axon to its target. Raising β flattens this gradient and thus reduces the effect of distance on competition in equation (29). Raising β thus causes the axonal distribution to become more isotropic with respect to distance.

Learning of Layer 2/3 Excitatory Horizontal Synaptic Weights

Once a horizontal axon reaches its target cell, then the strength of its synaptic connection can be modified by activity-dependent correlations. We use an instar learning law, which has become the standard law for learning self-organizing maps (Grossberg, 1976a, 1980b; Kohonen, 1989). During instar learning, the activity in the postsynaptic target cell turns on learning, and the adaptive weight learns the expected value of the presynaptic source cell's signals during intervals when the target cell is active. Disynaptic inhibition can prevent a postsynaptic cell from firing and thus, by instar learning, prevent the learning of irrelevant horizontal connections (Hess and Donahue, 1994). The synaptic weights V_{pqrijk} carried by the excitatory horizontal axons equal zero at the beginning of training, and are updated using the instar learning equation:

$$\frac{1}{\delta_V}\frac{\mathrm{d}}{\mathrm{d}t}V_{pqrijk} = z_{ijk}\Big[B\big(E_{pqrijk}\big)F\big(z_{pqr},\Gamma\big)U_{pqrijk} - V_{pqrijk}\Big] \qquad (33)$$

in which the synaptic weight V_{pqrijk} tracks the presynaptic signal $B(E_{pqrijk})F(z_{pqr},\Gamma)U_{pqrijk}$ at a rate proportional to its postsynaptic activity z_{ijk}. The binary function $B(E_{pqrijk})$ enables synaptic learning to begin when the axon begins to connect to the target cell:

$$B\big(E_{pqrijk}\big) = \begin{cases} 1 & \text{if } \big|1 - A\big(E_{pqrijk}\big)\big| < \varepsilon \\ 0 & \text{otherwise} \end{cases} \qquad (34)$$

Then V_{pqrijk} tracks the strength of the signal $F(z_{pqr},\Gamma)U_{pqrijk}$ from the source cell. At each position, there are four two-dimensional V_{pqrijk} kernels corresponding to the four orientational combinations of r and k. Figure 14*e*,*i* shows how the vertical-to-vertical V_{pqrijk} kernel has developed just before eye opening and after visual development self-equilibrates.

Development of Layer 2/3 Disynaptic Inhibitory Connections

Layer 2/3 disynaptic inhibition (Fig. 1*c*) is mediated by two weights. Weight T^{-}_{rijk} calibrates the mutual inhibition between layer 2/3 inhibitory interneurons in equation (28), and weight T^{+}_{rijk} calibrates the inhibition of layer 2/3 pyramidal cells by layer 2/3 disynaptic inhibitory interneurons in equation (26). These weights have only two spatial indices because they are short-range interactions whose spatial extent is limited to a single hypercolumn, indexed by (i,j). The indices r and k denote the orientations of the source cell and target cell, respectively. The weights start with zero values and develop using an outstar learning law (Grossberg, 1968, 1980b).

Outstar learning of inhibitory connections is used to maintain the balance between inhibition and excitation. Outstar learning accomplishes this by causing the inhibitory synaptic weights to track the expected activation of the excitatory cells. If instar learning had been used, then the inhibitory weights would have tracked the expected value of the inhibitory cells. If an excitatory cell got more and more active, this would not necessarily cause a balanced increase in inhibition. Instar learning of excitatory connections was used in (33) to offset imbalances in cell activation patterns while maintaining the selectivity of cell connections. Had outstar learning been used for that purpose, then problems could have ensued. For example, suppose that two cells, A and B, are learning excitatory connections to each other. Let cell A be active 90% of the time, and cell B be active 10% of the time. For simplicity, assume the activities are independent and always equal to one. If outstar learning were used, then the synaptic weight to cell A would approach 0.9, and the synaptic weight to cell B would approach 0.1. Therefore, the discrepancy between the cells would increase. Outstar learning at the horizontal layer 2/3 connections could hereby cause some cells to get stronger and stronger, and could end up using all the axonal resources to support connections to them, at the expense of other cells. However, with instar learning, the weight to cell A would approach 0.1, and the weight to cell B would approach 0.9, thereby reducing the discrepancy between their mutual activations, without a loss of selectivity. It is for these reasons that instar and outstar learning were used to control excitatory and inhibitory connections, respectively, in the model.

The outstar learning laws that are used to connect the inhibitory kernels T^{+} and T^{-} in equations (35) and (36) are:

$$\frac{1}{\delta_W}\frac{\mathrm{d}}{\mathrm{d}t}T^{+}_{rijk} = s_{ijr}\left[\tau\sum_{pqR}H_{pqRijk}F\big(z_{pqR},\Gamma\big) - T^{+}_{rijk}\right] \qquad (35)$$

$$\frac{1}{\delta_W}\frac{\mathrm{d}}{\mathrm{d}t}T^{-}_{rijk} = s_{ijr}\Big[s_{ijk} - T^{-}_{rijk}\Big] \qquad (36)$$

Here, both types of inhibitory weights track their postsynaptic activities at a rate proportional to their presynaptic inhibitory interneuron signal, s_{ijr}. In equation (35), the postsynaptic activity is $\tau\,\Sigma_{pqR}\,H_{pqRijk}F(z_{pqR},\Gamma)$ and in equation (36) the postsynaptic activity is s_{ijk}. Kernel T^{+} hereby tracks the activity $\tau\,\Sigma_{pqR}\,H_{pqRijk}F(z_{pqR},\Gamma)$ of the target pyramidal cell's apical dendrites, which is derived from layer 2/3 horizontal excitatory connections. Kernel T^{-} tracks the activity s_{ijk} of the target inhibitory interneuron. Figure 14*f*,*j* shows how the vertical-to-vertical T^{+} weight has developed just before eye opening and after visual development self-equilibrates, respectively. The vertical-to-vertical T^{-} weight develops similar values because the activity that it tracks, s_{ijk}, depends on $\Sigma_{pqR}\,H_{pqRijk}F(z_{pqR},\Gamma)$ in equation (28). The anisotropy that develops in these kernels helps to simulate psychophysical data about perceptual grouping (Grossberg and Raizada, 2000).

Development of Layer 4 Inhibitory Connections

The layer 4 surround inhibition (Fig. 1*b*) is mediated by W^{-}_{pqrijk} weights that carry mutual inhibition between layer 4 inhibitory interneurons in equation (25), and W^{+}_{pqrijk} weights that carry inhibition of layer 4 excitatory cells by layer 4 inhibitory interneurons in equation (20). These inhibitory weights start from zero values and develop using an outstar learning rule, in which learning is activated when the source cell turns on. During these sampling intervals, weight strength approaches the expected value of the target cell's activity at a rate that covaries with the source cell's activity. Such a learning law incorporates both Hebbian and anti-Hebbian properties (Singer, 1983), since weight strength can either increase or decrease to track and thereby balance its postsynaptic target activity. Inhibitory learning rules of this type have also been used to model dynamic receptive field changes produced by scotomas (Kalarickal and Marshall, 1999). The learning laws for the W^{-} and W^{+} weights are:

$$\frac{1}{\delta_W}\frac{d}{dt}W^{-}_{pqrijk} = m_{pqr}\big(m_{ijk} - W^{-}_{pqrijk}\big) \qquad (37)$$

$$\frac{1}{\delta_W}\frac{\mathrm{d}}{\mathrm{d}t}W^{+}_{pqrijk} = m_{pqr}\big(C_3 y_{ijk} - W^{+}_{pqrijk}\big) \qquad (38)$$

in which the inhibitory weights track their postsynaptic activities at a rate proportional to their presynaptic sampling signal, m_{pqr}. The postsynaptic activity is m_{ijk} in equation (37) and y_{ijk} (scaled by C_3) in equation (38). At each position, there are four two-dimensional W^{-} kernels and four two-dimensional W^{+} kernels, corresponding to each combination of vertical and horizontal connectivity, i.e. subscripts r and k in (37) and (38). Learning of $W^{\pm}_{pqrijk}$ is restricted to a local, circular window of sampled cells (i,j) around a source cell (p,q) such that:

$$D_{pqij} = \sqrt{(p-i)^2 + (q-j)^2} < W_{\text{range}}/2 \qquad (39)$$

All $W^{\pm}_{pqrijk}$ weights were initialized to zero at the beginning of training. To reduce the computational load, the kernels were averaged across spatial position after each integration step:

$$W^{\mp}_{pqrijk} = \frac{1}{N^2} \sum_{PQIJ} \delta\left[(p-i),(P-I)\right]\delta\left[(q-j),(Q-J)\right]W^{\mp}_{PQrIJk} \qquad (40)$$

where $\delta[a,b] = 1$ if $a = b$; $\delta[a,b] = 0$ otherwise, and N^2 is the number of cells in each layer. During training, $N = 30$. A similar approximation procedure was also used to compute spatial averages of the kernels U, V, T^+ and T^-. Figure 14*c*,*g* shows how the vertical-to-vertical kernel W^+ has developed just before eye opening and after visual development self-equilibrates, respectively. Kernel W^- develops in a similar way.

Parameters for the Developmental Equations (36) and (37)

Axon growth and synaptic weight update parameters are: $\delta_W = 1.0$, $C_3 = 6.0$, $W_{\text{range}} = 7$, $\delta_A = 0.25$, $U_{\text{total}} = 44.0$, $\psi = 0.01$, $\kappa = 6.0$, $\beta = 8.0$, $H_{\text{range}} = 11$, $\delta_V = 0.5$, $\varepsilon = 0.01$, $\tau = 1.5$.

Training Procedure

Model development occurred during two successive stages, as also occurs *in vivo*. The initial coarse specification of horizontal connections prior to eye opening is followed by a strengthening and increase in the selectivity of these connections after structured vision begins. The unstructured vision phase was modeled using uniformly distributed random noise inputs which are Gaussianly filtered to induce local correlations (Fig. 2, left). This Gaussian filtering uses the same standard deviation ($\sigma = 0.5$) that was used to define each lobe of the simple cell receptive field in equations (10) and (11). Following eye opening, inputs contain spatial structure that is determined by objects in the world. We modeled these structured visual inputs with randomly sized and positioned rectangles (Fig, 2, right), in keeping with the idea that essentially all visual objects have linear contours on a sufficiently small spatial scale. Rectangles were appropriate in the present simulation study because the model only represented horizontal and vertical orientations. Later work will use more orientations and will train the model using real-world images. In the present study, each input image contained seven rectangles, each with a contrast that was randomly distributed between 0 and 2. The length and width of each rectangle was determined by an iterative random process in which each dimension started at zero pixels, grew (independently) by one pixel at each iteration, and stopped growing with probability 0.1 at each iteration. The images were processed with wrap-around in both the x and y dimensions in order to avoid spurious boundary effects.

The training procedure consisted of presenting each randomly generated image (see Fig. 2) and integrating cell activation equations (3)–(28), using the fourth-order Runge–Kutta method, until equilibrium, while keeping all the weights fixed. Equilibrium was considered achieved when the average absolute activity change of layer 2/3 pyramidal cells, defined in equation (26), fell below a threshold of 0.002. This typically occurred after ~20 iterations through equations (3)–(28). Then, a single integration step of the developmental equations (36) and (37) was run using the fourth-order Runge–Kutta method. This scheme captured the main idea that development occurs slowly relative to the time-scale of cell activation. Using this procedure, the network was trained with 20 000 unstructured images (Fig. 2, left) followed by 30 000 structured images (Fig. 2, right). After presentation of ~10 000 unstructured images, the learning equations stabilized, and little change took place until the structured images were presented. A burst of new learning then took place due to the different statistics of the structured images, and did not stabilize until presentation of ~15 000 structured images.